Thermal Diffusivity and Freeze Thaw Behavior of Pervious Concrete Pavements

A THESIS
SUBMITTED TO THE FACULTY OF THE GRADUATE SCHOOL
OF THE UNIVERSITY OF MINNESOTA
BY

Alexandra Kamilla Akkari

IN PARTIAL FULFILLMENT OF THE REQUIREMENTS
FOR THE DEGREE OF
MASTER OF SCIENCE

Dr. Randal J. Barnes

December 2014

ACKNOWLEDGMENTS

I would like to thank my advisor, Dr. Randal J. Barnes, for his continued assistance, guidance, and patience during my graduate career at the University of Minnesota. His unparalleled expertise in advanced mathematical modeling for such a broad range of specialties in civil engineering inspired my initial interest in this research and, more importantly, made the results of this thesis possible. His sincere passion for teaching and mentoring of students has been influential to me since my undergraduate days, and I would not be where I am today without his support.

I would also like to thank my former colleagues from MnDOT for their support of my graduate studies and assistance with this thesis. Dr. Bernard Izevbekhai's vast knowledge of all things concrete pavements proved to be invaluable to the development of this thesis. I am very thankful to have had his mentorship in my professional growth. I would also like to thank Maureen Jensen for making graduate school a possibility while I worked full time. Finally, I would like to thank Steve Olson, Len Palek, and Ben Worel for their significant contributions to this research.

ABSTRACT

Past research has found that pervious concrete pavement may have significantly different thermal behavior than comparable impervious concrete pavements, which may lead to differences in important physical characteristics such as freeze-thaw behavior. This research analyzes in-situ temperature data collected from multiple pervious and impervious concrete pavement test sections over a four-and-a-half-year period. Objectives include determining in-situ thermal diffusivity of pervious concrete pavements, changes in thermal diffusivity over time due to deterioration and maintenance events, and frequency of freeze-thaw cycles in pervious concrete pavements compared to impervious concrete pavement.

Research results were achieved through the development of multiple programs written for MATLAB. The first program performs an optimization routine to solve for thermal diffusivity, utilizing the heat equation to fit a temperature gradient to the raw data. This program was validated using synthetic data. A second program was developed to perform an uncertainty analysis on the thermal diffusivity results. The final portion of this research applied two previously developed methods for counting freeze thaw cycles, the 0°C Method and the Max/Min method.

The analysis shows that pervious concrete pavements have a significantly lower in-situ thermal diffusivity than comparable impervious concrete pavements. The fitted thermal diffusivity of impervious concrete was consistent with those found in laboratory studies. Results showed notable seasonal trends in the thermal diffusivity results. There was no observed change in thermal diffusivity following a limited number of maintenance events. The uncertainty analysis found the standard deviation of errors and standard deviation of thermal diffusivity to be significantly low, supporting the validity of the model and the fitted thermal diffusivities. The 0°C Method showed reduced freeze-thaw cycles in the pervious concrete pavements compared to the impervious concrete pavement. However, the Max/Min method resulted in an almost equal number of cycles for both pavement types. Therefore, further analysis of pervious concrete pavements using new methods for detecting freeze thaw cycles would be beneficial.

TABLE OF CONTENTS

LIST OF FIGURES

LIST OF TABLES

CHAPTER 1: INTRODUCTION

1.1 Definition of Pervious Concrete

Pervious concrete, the primary subject of this thesis, is a material which differs from common Portland cement concrete (PCC) primarily in its air void structure. In contrast to typical Portland cement concrete mixtures, pervious concrete mixtures contain little or no fine aggregate (Shu et al, 2011). This open gradation of pervious concrete mixtures creates highly interconnected voids within the matrix, leading to a high water permeability and porosity (Wu et al., 2011). The water and cementitious content in pervious concrete is also specifically proportioned to obtain only a thin layer of paste coating the coarse aggregate, with large air voids between aggregate solids. These large voids in pervious concrete differ from both the entrained air, created from the use of admixtures, and the entrapped air, caused from improper mixing or consolidation, found in typical Portland cement concrete (Goguen, 2012). The air void content in pervious concrete typically ranges from 15 to 35% of the volume (Vancura et al, 2011). Studies have found that void contents within this range can lead to a water permeability ranging from 2-6 mm/s (Huang et al., 2010).

Initial research on pervious concrete generally had shown that as air void content increases, both freeze thaw durability and strength decrease (CTRE IOWA STATE, 2006). It was also found that saturated voids in a typical pervious concrete mix with no fine aggregate would result in deterioration during a freeze thaw event (Mata, 2008). However, many more recent studies have been done to develop pervious concrete mixture designs that address these issues. For instance, Kevern et al. found that pervious concrete made with coarse aggregate with absorption below 2.5% and a specific gravity above 2.5 may perform well in high traffic and hard freeze/thaw environments. It is common to also include air entrainment within the concrete mixture to address freeze-thaw concerns (Henderson et al., 2012). Other studies have found that including only minimal amounts of fine aggregate can improve the freeze-thaw durability, but may also reduce permeability (Vernon, 2006).

1.2 Pervious Concrete Pavements

Pervious concrete is most commonly used as a material in paving applications, such as parking areas, driveways, trails and streets with low traffic volumes (Washington Aggregate and Concrete Association). Pervious concrete pavement systems typically consist of a full depth pervious concrete surface layer above a stone base layer (American Concrete Pavement Association). The air void structure and high permeability of pervious concrete allows water to pass through the surface layer of the pavement and into the base layer. Consequently, the stone base layer acts as a reservoir for water as it infiltrates into the surrounding soil (American Concrete Pavement Association). The thickness of the reservoir base layer is determined by both structural requirements and hydrological design processes (Virginia Department of Environmental Quality). Other common features of pervious concrete pavement systems include geotextiles, used as a means of separating base layers from the subgrade, and drain pipes, used to direct surplus water from large-volume events to nearby catch basins (Minnesota Pollution Control Agency). There are many other types of pervious pavement systems, including porous asphalt pavements, interlocking concrete or permeable pavers, and plastic or concrete grid systems with gravel-filled voids (City of Los Angeles). However, the work in this thesis will only focus on pervious concrete pavements.

Although the large pore size of pervious concrete provides many benefits in pavements, it also allows for small sediment particles to enter the pavement surface, which eventually clog the pavement and hinder the hydrological performance of the material (Radlińska et al., 2012). For this reason, pervious concrete pavements require regular maintenance (Radlińska et al., 2012). Commonly practiced maintenance methods include vacuuming, sweeping, power blowing, pressure washing and rinsing (Henderson et al., 2011). Suozzo et al. suggest that maintenance should begin soon after construction, as their research has shown that vacuuming is not nearly as effective at restoring infiltration rates after two years of service, compared to results from vacuuming within the first year of service (Suozzo et al., 2012). One study of eight different pervious concrete pavement sites with between six and twenty years of service found that pressure washing, vacuuming,

sweeping, or a combination of the three can increase infiltration rates of clogged pervious concrete pavements by 100%, 90% and 200%, respectively (Wanielista et al., 2007).

1.3 Benefits of Pervious Concrete Pavements

Population growth and urbanization is rapidly increasing the amount of impervious surface area (Ferguson, 2005). This in turn can cause excess stormwater runoff and bank erosion, and transport pollutants into natural water supplies (Sonebi, 2013). Pervious concrete pavements can address these issues by allowing stormwater to flow through the pavement surface and permeate the underlying soil, providing a natural filtration method and reducing the amount of pollution to the environment (United States Environmental Protection Agency, 2014). Besides reducing runoff and pollution treatment, pervious concrete pavements can help to recharge aquifers, encourage tree growth, and even provide a cost savings by eliminating the need for separate drainage structures (Lemay et al., 2011).

In addition, it is believed that pervious concrete pavements have the ability to mitigate the heat island effect (Wong, 2005). The heat island effect refers to a large thermal difference between developed (or paved) and undeveloped areas. This thermal difference causes harmful effects on the surrounding microclimate, as well as human and wildlife habitat (Ashley, 2008). The material behavior of pervious concrete pavements contributing to this phenomenon is complex. One article attributed the possible gradient reduction to the ability of pervious concrete to allow moisture from subsurface layers to evaporate and cool the concrete while simultaneously absorbing less heat due to the reduced thermal mass of the material (Towner, 2008). To describe the behavior in more detail, the presence of larger air voids in pervious concrete pavements increases the surface area which reduces heat transfer to the lower pavement structure and soil and, in turn, reduces bulk heat storage (Wong, 2005). This stored heat, a significant contributor to the urban heat island effect in cities, is thereby reduced at night. Some studies found that pervious concrete pavements can also reduce the heat island effect due to the light grey coloring of the material (Henderson et al., 2012).

1.4 Pervious Concrete Pavements in Cold Weather Regions

Pervious concrete pavements have long been used as a method of stormwater management and to address environmental concerns in warm-weather regions, with parking lot and commercial applications dating back well over 20 years (Michigan Concrete Association). However, pervious concrete pavements have only recently become popular in cold-weather regions, where harsh climates can provide additional challenges (Chen et al, 2013). Although pervious concrete pavements are designed to allow water to flow through the pavement, there are many circumstances under which the pavement may become fully saturated. Poorly draining bases, improper subbase preparation, and harsh climates that experience precipitation while temperatures are below freezing for long periods can all cause moisture to be retained in pervious concrete pavements (Portland Cement Association, 2014). In a fully saturated state, pressure can build during freezing that can break down the very thin paste that encapsulates the aggregate in pervious concrete (NRMCA, 2004). It is believed that this phenomenon can cause severe raveling, or disintegration, of the surface layer of pervious concrete pavements (Rohne, 2009).

As explained in detail in Chapter 3 of this report, thermal diffusivity is defined as the rate at which temperature changes are made in a material. Literature review found pervious concrete may have a lower thermal diffusivity than standard impervious concrete (Lamond et al., 2006 and Carlson, 2011). Therefore, pervious concrete may be able to reduce the number of freeze thaw cycles or reduce the depth of daily freezing and thawing cycles, as temperature changes will not occur as quickly as they would in impervious concrete pavements. For example, pervious concrete may stay frozen throughout the winter months even if ambient daytime temperatures rise above freezing. In addition, the frost line may take longer to extend the full depth of the pavement when ambient temperatures drop below freezing. This research will investigate these theories further.

1.5 Case Studies Relating to Thermal Behavior of Pervious Concrete Pavements

The advantages and disadvantages of using pervious concrete in pavements discussed in the previous sections are dependent on a wide range of material properties. Due to the large differences in air void structure and material composition between pervious concrete and typical Portland cement concrete, it is expected that the two materials would also have significantly differing thermal properties. The specific material property of thermal conductivity may be able to indicate whether PCC pavements will have significantly different thermal behavior than pervious concrete pavements. Thermal conductivity, the property most commonly used to quantify the ability of a solid to conduct heat, is defined as the rate at which heat energy flows through a material normal to the temperature gradient (Shindé, 2006). Much research has shown that the thermal conductivity of concrete is influenced by the mix proportions, micro-cracks, void structure, aggregate types, and unit weight (Tang et al., 2012). One laboratory study found that Portland cement concrete has a thermal conductivity of 1.83 W/m°C, whereas pervious concrete has a thermal conductivity of 1.04 W/ m°C, almost half that of PCC (Kaloush, 2009). The work in this thesis determines if similar results for thermal conductivity of pervious concrete pavements can be found using in-situ data.

In contrast to the potential disadvantages of using pervious concrete in pavements in cold-weather regions discussed in section 1.4, one study suggested that pervious concrete pavements may undergo less-frequent freezing and thawing cycles compared to a typical PCC pavement in the same environment (Rohne, 2009). The study suggested that the large air voids in pervious pavement may have an insulating effect and keep the pavement at a more consistent winter temperature than that of the subgrade. It was theorized that less frequent freeze-thaw cycles could counterbalance the reduced freeze-thaw durability and allow pervious concrete pavements to perform comparably to impervious pavement types. However, this study was performed on limited test data, leaving a need to validate these conclusions.

Another study done in 2013 monitored the temperature of five different types of pervious concrete pavements over a year-long period. It also concluded that sub-base temperature

fluctuations were reduced when compared to the base layer due to the insulating capacity of the pervious pavements (Novo et al, 2013).

A study performed in Iowa in 2011 monitored the temperature of a traditional concrete pavement system alongside a pervious concrete pavement system. This study had many noteworthy conclusions: (1) The pervious concrete pavement system cooled faster after heat waves and spikes, which could reduce heat-related illnesses and spikes in energy demand; (2) although the pervious concrete system was generally cooler in the summer months, it retained heat longer into the winter months, which could be explained by the insulating effect of the voids; and (3) the design of the concrete layers of pervious concrete pavements has a much larger impact on the heat capacity of the system than the depth of the base layers (Hasebach et al., 2011).

One study performed in Tennessee in 2007 monitored the temperature and moisture in twelve different pervious concrete pavement plots over a winter season. Although not in a harsh freeze-thaw environment, the results of this study provided interesting insight into the thermal performance of pervious concrete pavements. The monitoring showed that although the ambient temperature dropped below freezing 24 times, with the coldest being -9.9 degrees Celsius, these freezing events never occurred when there was moisture present in the pavements. This was attributed to the fact that water increases the thermal capacity of the system. In addition, the pervious concrete never reached a temperature below the ambient air temperature and the base layer was even further insulated, never reaching temperatures below freezing (Tyner et al., 2009).

Another study performed by Iowa State University in 2007 also monitored pervious concrete pavement and traditional concrete pavement in a side-by-side test setup. The results from this study led to the conclusion that air in the aggregate base layer acts as an insulating layer. In addition, it was suggested that there is a higher latent heat level in pervious concrete pavement systems due to a higher soil moisture content. The combined effect of these two conditions could delay, and possibly prevent, a layer of frost from forming under the pervious concrete, therefore maintaining the permeability of the pavement system. Another significant finding was that thaw in the base layers occurred

one month earlier in the pervious concrete pavement than the traditional concrete pavement (Kevern et al., 2009).

1.6 Research Need and Objective

The research noted in section 1.5 provides useful information on how the thermal properties of pervious concrete may impact the freeze-thaw behavior in pavements. In continuation of these studies, the work in this thesis analyzes pervious concrete pavements over a much longer period to assess any changes in these behaviors over time. It establishes whether trends and behaviors are a response to the conditions present during a single season, or are prevalent over many continuous seasons. In addition, this research helps to clarify areas of uncertainty where results from previous studies disagreed on important matters.

The research in this thesis analyzes in-situ temperature data collected from multiple pervious and non-pervious concrete pavement test sections for three main purposes:

1. to verify, or falsify, results found in past laboratory studies;
2. to quantify the thermal conductivity; and
3. to characterize temperature gradients and freeze-thaw behavior of pervious concrete pavements.

Specific deliverables of this research include the following: 1) In-place thermal diffusivity of three different types of pervious concrete pavements; (2) trends in thermal diffusivity over time to identify any impact from changes in the air void structure due to deterioration, clogging or vacuuming maintenance events; (3) frequency of freeze-thaw cycles in pervious concrete pavements compared to standard PCC pavements; and (4) insight on the ability of pervious concrete to reduce freeze-thaw cycles in underlying base layers.

CHAPTER 2: TEST CELLS AND DATA COLLECTION

2.1 Description of Test Facility

This research analyzed data collected from five pavement test cells located at the MnROAD test facility. MnROAD, located in Monticello, Minnesota, is a pavement test track consisting of over 35 test cells, each with a distinct pavement type and design (Khazonivich et al., 2013). Most of the test cells are located on either the Mainline or Low-Volume Road sections; however, additional test cells off the two main roadway segments have also been constructed to test different traffic load rates and vehicle types.

The Mainline is a 3.5-mile segment of Interstate 94, which carries live traffic approximately 26,400 vehicles per day. The Low-Volume Road (LVR) at MnROAD consists of a two-and-a-half-mile closed loop, two-lane roadway containing 20 test cells (Wilde, 2013). The purpose of the LVR is to mimic traffic conditions of rural roads. Therefore, traffic on the LVR is restricted to a single 19-wheel, five-axle tractor with trailer that travels on the inside lane only, leaving the outside lane subject only to environmental loads (Lebens et al., 2012). The tractor, which is operated by MnROAD staff, completes approximately 80 laps per day around the LVR. Test cells are also located on the south side of the MnROAD pole barn. Portions of the original bituminous pavement parking lot in this location were replaced with pervious concrete pavement test cells. They act as the driveway to the pole barn and receive small daily traffic loads.

Each test cell is frequently monitored for its response to both traffic and environmental conditions over time. Over 5,000 electronic sensors installed in the pavement test sections measure dynamic load response, environmental strain, moisture, temperature, surface layer deflections and more. Frequent nondestructive testing is also performed to measure ride quality, sound absorption, noise, faulting, rutting, skid resistance, texture, and many other properties that contribute to pavement performance.

2.2 Description of Test Cells

Five MnROAD test cells were evaluated in this research. Four of these test cells are pervious concrete pavements. The fifth test cell is a standard Portland cement concrete

(PCC) pavement, which was included as a control cell. As thermal properties of standard Portland cement concrete pavements have been previously studied and are well understood, results from the analysis of this test cell will help to validate the accuracy of the methods used in this research.

Cells 85 and 89 – Full-Depth Pervious Concrete Pavement

Two of the test cells evaluated, cells 85 and 89, are full-depth pervious concrete pavements located on the Low-Volume Road. These test cells were designed using both structural and hydrological design processes. This included the use of the Mechanistic Empirical Design Guide (using data from an existing pervious concrete test cell at MnROAD), structural analysis using ISLAB software, as well as the development of a hydrological infiltration model for pervious concrete (Bernard's Tortuosity Model) (Izevbekhai et al., 2011). The results of this design process produced the desired performance requirements of a porosity between 15 and 18%, unit weight less than 135 pcf, and seven-day flexural strength of 300 psi.

The structural design of both cells 85 and 89 included a 7-inch-thick pervious concrete pavement surface layer. The pavement layer was placed over 4 inches of railroad ballast and 8 inches of a gap-graded base to facilitate drainage. The difference between cells 85 and 89 is in the subgrade conditions. Cell 85 utilizes a full infiltration scenario with a granular subgrade. In contrast, Cell 89 develops a retention system through the use of a cohesive clay subgrade.

Cells 85 and 89 were constructed in October of 2008. The test cells were paved using a fix-form paver system and compacted with a steel drum roller. They were the first cells at MnROAD to have a curb and gutter system.

Cell 39 – Pervious Concrete Pavement Overlay

Cell 39 is the third pervious concrete pavement test cell located on the Low-Volume Road. The pervious concrete mix design for Cell 39 was developed by Iowa State University's National Concrete Pavement Technology Center. This included extensive trial batching at American Engineering Testing. The mix was designed to be self-

consolidating. This pervious concrete mix was unique in the fact that it utilized polyolefin fibers, nonfibrous polymers. The pervious concrete had a design compressive strength of 2,500 psi at seven days, an ultimate flexural strength of 450 psi, and an overlay bond strength of around 300 psi. By using a design void content of 22.5%, the finished pavement was to achieve a permeability of over 500 in/hr.

This test cell consists of a 4-inch-thick pervious concrete pavement overlay placed above a 6-inch thick existing PCC substrate pavement layer. The existing base and subgrade layers consisted of 5 inches of Class 5 aggregate base, and a clay subgrade.

Construction of Cell 39 began in October of 2008 along with cells 85 and 89. The pavement was also placed using fixed-forms and roller compaction with vibratory drums. Unlike cells 85 and 89, French drains consisting of CA15 were installed along the shoulders of Cell 39 with drainage routes at 50-foot intervals to facilitate drainage.

Cell 64 – Pervious Concrete Pavement Driveway

The fourth pervious concrete pavement test cell evaluated in this research was Cell 64. Cell 64 is a 60-foot by 16-foot pervious concrete pavement driveway located at the entrance to the MnROAD pole barn. As this test cell was one of the first uses of pervious concrete pavement in Minnesota, there were still many unknowns when designing the mix proportions. Therefore, the test cell was divided into three sub-cells that differed in the pervious concrete mix design to allow for comparison in performance. The three pervious concrete mixes mainly differed in the type and gradation of coarse aggregate. A low water-to-cement ratio of 0.27, along with admixture type and dosage, was held constant in all mixes. No fine aggregate was used in any of the four mixes. Water, fly ash, and cement content only varied slightly. The pervious concrete was designed for an anticipated 33% air content and zero slump.

Similar to the full-depth cells placed on the Low-Volume Road, Cell 64 consists of a 7-inch-thick pervious concrete pavement layer, a 12-inch-thick CA-50 aggregate base, and clay subgrade. CA-50 is a MnDOT designation for coarse aggregate with ¾” nominal

maximum size. A 2-inch-diameter pipe was placed beneath the driveway to facilitate drainage of water flowing through the pavement structure.

The driveway was constructed in late September of 2005. Placement involved the use of a pneumatic roller screed.

Cell 52 –Full-Depth Portland Cement Concrete Pavement (Control)

The final test cell included in this research is Cell 52. Cell 52 is included as the control, non-pervious test cell. The Portland cement concrete used in this test cell had a design air content of 5.5% and a water-to-cement ratio of 0.46. The test cell is a 7.5-inch- thick jointed plain concrete pavement placed over 5 inches of aggregate base material. The transverse joints in Cell 52 contain four different types of dowel bars, including two types of epoxy-coated steel dowels and two types of fiber-reinforced polymer (FRP) dowels.

Cell 52 was constructed in 2000 and is located on the MnROAD Low-Volume Road. The research objectives for Cell 52 included determining the load response behavior and durability of FRP dowel bars, as well as characterization of early-age and long-term concrete pavement behavior. Therefore, the necessary temperature measurements required for the analysis in this research has been collected since construction.

Cell 54 – Full-Depth Impervious Concrete Pavement

Cell 54 was included in this research to provide supplemental comparison data for freeze-thaw cycle analysis only. The concrete in this test cell was made using Mesabi-Select coarse aggregate. The test cell consists of an 8-inch-thick surface layer with a variable-depth Class 5 aggregate base.

The test cell was constructed in the fall of 2004 on the MnROAD Low-Volume Road.

2.3 Thermocouple Sensors and Data Collection

The data used to evaluate the thermal properties of the concrete pavement test sections in this research was collected using thermocouple sensors. All five test cells were thoroughly instrumented at the time of construction with electronic thermocouple

temperature sensors at different depths throughout the concrete pavement, base, and subgrade.

Thermocouple sensors measure the temperature of a material in which they are embedded. Thermocouple sensors consist of a pair of two different metal alloy wires, commonly copper and constantan, which are connected near the point of desired temperature measurement. [1] Temperature measurement using thermocouples is based off the principle that when two dissimilar metals are joined together an electromotive force (e.m.f.) that is a function of the absolute temperature is generated (Morris, 2012). This principle is commonly referred to as the Seebeck effect. The Seebeck voltage is an open-circuit voltage that is proportional to the difference in temperature between the point of interest (hot junction) and the reference open end (cold junction) of the wires (Van Herwaarden et al., 1986).

Temperature data from the thermocouple sensors in the MnROAD test cells described in section 2.2 is automatically collected at a defined interval and sent through carefully placed wires to be stored in an electronic database. MnROAD uses Type-T thermocouple wires manufactured by Omega. The thermocouples are fabricated into "trees" by MnROAD staff, allowing temperature data to be collected at varying depths throughout the pavement, base, and subgrade layers at a single location. This vertical "tree" mounting method allows for vertical temperature profiles to be determined. These are important in understanding the material properties of the pavement and base layers. The thermocouple sensor trees are securely mounted in the base material and concrete is carefully hand-placed and compacted around the tree before full paving of the test cell to avoid damage to the sensors. A photograph of a thermocouple tree in place before paving has occurred is shown in Figure 1.

Figure 1: Thermocouple Tree

One thermocouple tree was installed in both cells 85 and 89. Both of these trees consisted of 16 sensors at increasing depths, with five in the pervious concrete pavement layer, one in the railroad ballast base material, two in the CA-15 base material, and eight in the subgrade (sand and clay for cells 85 and 89, respectively). Since installation, these sensors have been collecting temperature data at all sensor depths at 15-minute intervals.

Three thermocouple trees are currently collecting data in Cell 39. Two trees are still operating since they were installed in 1993 in the existing substrate PCC pavement. The third tree was installed during construction in 2008. This tree consisted of five sensors at different depths in the pervious concrete pavement overlay; four additional sensors were retrofitted into the underlying existing PCC pavement substrate. All thermocouple sensors in Cell 39 collect temperature data in 15-minute intervals.

There are two thermocouple trees installed in Cell 64. Each of these trees consists of eight thermocouples at varying depths, with four sensors in the pervious concrete pavement layer, one sensor in the stone base, and three sensors in the clay subgrade. Unlike the other test cells evaluated in this research that provide data every 15 minutes, the sensors in Cell 64 have been collecting temperature data in one-hour intervals since construction. Although there is less frequent data for this test cell, the full analysis was still conducted and the accuracy of the results was validated with uncertainty statistics in Chapter 6.

Finally, Cell 52 has two thermocouple trees. Each tree has six sensors in the concrete pavement layer, one in the stone base, and one in the clay subgrade. Again, these sensors collect data every 15 minutes.

The detailed sensor locations for each of the five test cells, including the depth, station and offset of each thermocouple, can be found in Appendix X of this report.

The period of data analyzed in this research spans from October 2008, when cells 85 and 89 were constructed, to March 2013. This four-and-a-half-year period of data was selected in order to include five full winter seasons where freeze-thaw cycles could be evaluated.

CHAPTER 3: DEVELOPMENT OF DIFFUSIVITY MODEL

3.1 Heat Transfer Theory

As described in Chapter 1, one of the most common properties used to measure the thermal behavior of concrete is the thermal conductivity (k), or the rate at which heat flows through the material. However, a related property, known as the thermal diffusivity (α), can be directly calculated using the thermocouple temperature data described in the Chapter 2.

Thermal diffusivity is defined at the rate at which temperature changes are made in a material, and can be thought of as the thermal inertia with units of area per time (Venkanna). A higher thermal diffusivity will cause a material to approach thermal equilibrium with its surroundings faster (Thirumaleshwar, 2009). In other words, higher thermal diffusivity can allow faster propagation of heat into the material. Although, thermal diffusivity (α) is related to temperature and thermal conductivity is related to heat (k), the two properties are directly related by a constant known as the specific heat capacity (c_p) as well as the density (ρ) of the material (Tritt, 2004). Specific heat capacity is the ability of a medium to store heat for a fixed unit rise in temperature and unit mass. (Kaviany, 2002) The relationship between the four properties discussed is expressed in the equation below.

$$\alpha = \frac{k}{\rho c_p}$$

The method used to determine the thermal diffusivity of the pervious concrete pavement test cells and the typical Portland cement concrete pavement test cell was to apply the heat equation to the available thermocouple data described in Chapter 2. The heat equation, one of the most important tools in conduction analysis, is a parabolic partial differential whose solution can provide the temperature distribution $T(x,y,z)$ in a medium as a function of time. (Incropera, 2011) The three dimensional form of the heat equation for a medium of constant thermal conductivity is given below, where T is temperature, t

is time, $\dot{q}$ is the rate of energy generation per unit volume, and x, y, and z are the three special variables.

$$\frac{\partial T}{\partial t} = \alpha\left(\frac{\partial^2 T}{\partial x^2} + \frac{\partial^2 T}{\partial y^2} + \frac{\partial^2 T}{\partial z^2} + \frac{\dot{q}}{k}\right)$$

To apply this equation to the available thermocouple data, it must first be simplified to one dimension. This will allow analysis of the temperature variation (or gradient) across the depth of the thermocouple tree over time.

The one dimensional heat equation is often derived by considering a metal rod with a non uniform temperature (T) across its length (x). The rod must be considered thermally insulated in the lateral direction and sufficiently thin such that temperature can only flow along the length of the rod. (Bray, 2012) In this case, heat will transfer from regions of higher temperatures to regions of lower temperatures. Then, three basic physical principles are applied to form the heat equation. First is Fourier's Law of Heat Conduction, which states that the rate of heat flow through a homogeneous solid is directly proportional to the temperature gradient causing the heat flow and the area *A* normal to the direction of the heat flow, mathematically expressed in the equation below (Thirumaleshwar, 2009):

$$Q = Rate\ of\ heat\ flow = -kA\frac{\partial T}{\partial x}$$

Next, if you consider an infinitesimally thin slice of the rod with width *Δx*, and corresponding infinitesimal mass *Δm*, the heat energy stored in the element can be defined with the following equation (Banerjee, 2014):

$$Heat\ energy = c_p \Delta m T$$

The temperature throughout the slice can be defined as a function of both position *x* and time *t*, *u(x,t)*. Then, for a cross-sectional area A, the heat energy can be further described as follows:

$$Heat\ energy = c_p \times \rho A \Delta x \times T = c_p \rho A \Delta x T(x,t)$$

Then, by the Law of Conservation of Energy, the change of heat energy in a segment in time *Δt* is equal to the difference between heat in from the left boundary and the heat out from the right boundary (Fulford, 2002). Using this law and combining the above equations produces the following:

$$c_p \rho A \Delta x T(x, t + \Delta t) - c_p \rho A \Delta x T(x, t) = \Delta t A \left(-k \frac{\partial T}{\partial x}\right)_x - \Delta t A \left(-k \frac{\partial T}{\partial x}\right)_{x+\Delta x}$$

Rearranging, with ρ, c_p, A and k all constant throughout the material:

$$\frac{T(x, t + \Delta t) - T(x, t)}{\Delta t} = \frac{k}{c_p \rho} \left(\frac{\left(\frac{\partial T}{\partial x}\right)_{x+\Delta x} - \left(\frac{\partial T}{\partial x}\right)_x}{\Delta x} \right)$$

Therefore, taking the limit of the above equation as Δt and Δx go to zero for an infinitesimally thin section at a point in time produces the one-dimensional heat equation, listed below in terms of either the thermal conductivity or thermal diffusivity, respectively:

$$\frac{\partial T}{\partial t} = \frac{k}{c_p \rho} \left(\frac{\partial^2 T}{\partial x^2} \right)$$

$$\frac{\partial T}{\partial t} = \alpha \left(\frac{\partial^2 T}{\partial x^2} \right)$$

The final equation listed will be used in the analysis throughout the remainder of this report.

3.2 Modeling Partial Differential Equations in MATLAB

Modeling the partial differential heat equation to solve for thermal diffusivity required the use of MATLAB programming software to perform the high-level numerical computation, as well as to construct visualization of the results. The program *DiffuModel* was written specifically for this research to address items number 1 and 2 listed in section 1.6. When *DiffuModel* is run in MATLAB, it conducts an optimization process that

solves for the thermal diffusivity of the pavement given a specific subset of pavement temperature data.

Two functions built in to the MATLAB software were significant contributors to the analysis process: *pdepe* and *fminbnd*. To give a very general overview of the process included in the *DiffuModel* program, the *fminbnd* function was run to find the thermal diffusivity which would generate a temperature gradient that best fit the actual in-situ temperature data at the middle sensors. The *fminbnd* function preforms an iterative search for the optimal thermal diffusivity by calling on the *pdepe* function for each test diffusivity value. The *pdepe* function accepts temperature data from the top and bottom sensors in the pavement over time, temperature data at all sensor depths taken at time zero, and calculates predicted temperatures at all other depths and time given a specified thermal diffusivity.

The *pdepe* function solves initial-boundary value problems for parabolic elliptic partial differential equations in three dimensions. The differential equations must follow the form shown in the equation below.

$$c\left(z,t,T,\frac{\partial T}{\partial z}\right)\frac{\partial T}{\partial t} = z^{-m}\frac{\partial T}{\partial z}\left(z^{m}f\left(z,t,T,\frac{\partial T}{\partial z}\right)\right) + s\left(z,t,T,\frac{\partial T}{\partial z}\right)$$

In this equation, m is a parameter corresponding to the symmetry of the problem, with m equal to 0 for a slab, 1 for a cylindrical shape, or 2 for a spherical shape. To transform the above equation to follow the one-dimensional heat equation, the constant m is set equal to zero. The functions *c*, *s*, and *f* were defined as follows:

$$c\left(z,t,T,\frac{\partial T}{\partial z}\right) = 1$$

$$s\left(z,t,T,\frac{\partial T}{\partial z}\right) = 0$$

$$f\left(z,t,T,\frac{\partial T}{\partial z}\right) = \alpha\frac{\partial T}{\partial z}$$

$$\alpha = Thermal\ Diffusivity$$

$$T = Temperature$$

$$z = Pavement\ depth$$

Once the partial differential equation has been defined in this manner, the pdepe function implements the method of lines to solve the partial differential equation in one space variable and time (Shampine et. al, 2003). The method of lines uses discretization in space to obtain algebraic approximations to the second order partial derivative term in the heat equation (Schiesser, at al., 2009). As a result of this process, the spatial derivatives are no longer stated in terms of the spatial independent variable, leaving time as the only remaining independent variable. This results in a system of ordinary differential equations that can be integrated across time to obtain a solution.

The *pdepe* function is written to accept six specific input values. The first two are described above: m, and a handle to the function f which is defined separately in the *DiffuModel* program. A function handle in a MATLAB program allows you to invoke a separate function regardless of where it is called from. Two additional function handles are accepted as inputs: one defining the boundary conditions and one defining the initial conditions. The final two inputs, "xmesh" and "tspan" refer to a vector along the z direction (where z is defined as pavement depth in the program) and a vector across time, respectively. Together, "xmesh" and "tspan" define the grid points for which solutions to the partial differential equation are being requested. Through these definitions, the *DiffuModel* program utilizes the pdepe function output to generate a three-dimensional temperature profile of the pavement.

3.3 Boundary Conditions

As stated above, the boundary conditions required by the program to solve the partial differential heat equation for thermal diffusivity are the temperatures over time in both the top and bottom sensors in the concrete pavement layer. However, *pdepe* automatically selects a time interval over which to perform the integration. This time interval may be more frequent than the 15minute (or one-hour) intervals at which the sensors are set to

collect data. Therefore, a second embedded function was written in to the *DiffuModel* program which automatically interpolates between the temperature measurements to create a boundary value at every interval that *pdepe* automatically selects. The *spline* option in MATLAB was used to perform this interpolation, which uses cubic spline interpolation to fit a piecewise polynomial to the data. This helps account for the wave shape in the temperature variation more accurately than would linear interpolation.

3.4 Initial Conditions

Before specifying the initial conditions, a vector must first be defined that specifies the points, or depths, at which a numerical solution will be requested over time. The accuracy of the modeled solution produced by the *pdepe* function depends highly on the fineness of the mesh. However, a finer mesh also significantly increases the required computing time. Therefore, the program was adjusted specifically for the subsets of data to be analyzed in this research by performing a trial run stage where different mesh sizes were tested to optimize accuracy and computing time. The results showed that a mesh size of each sensor depth plus another 20 depths evenly spaced between the top and bottom sensors in the pavement would produce the best results. Then, the initial condition was defined in the program as the temperature at all depths in the mesh at time zero. This again requires interpolation between the temperatures at the sensor depths. To do this, a third embedded function was written in to the program in which the *spline* option in MATLAB's interpolation function was used to automatically define the initial temperatures. This information was passed to the *pdepe* function as an input using a function handle.

3.5 Optimization Process

The processes above describe how the parabolic partial differential equation function (*pdepe*) in MATLAB is built upon in the *DiffuModel* program to model the heat equation and thermal gradient throughout the pavement depth given boundary conditions, initial conditions, and a specified value for thermal diffusivity. Additional steps were needed to use the generated model to solve for a thermal diffusivity that produces a time-dependent temperature gradient that best fits the data collected from the thermocouple sensors. The

fminbnd function in MATLAB is utilized to search for a thermal diffusivity, within a specified range, that best fits the actual data by searching for a value that minimizes the error. This is done by varying the diffusivity by a small amount, resolving the partial differential equation, and then calculating the error between the generated solution and the data measurements at the middle sensors at each 15-minute (or one-hour) interval. Then, the *DiffuModel* program calculates the root mean squared error between the modeled temperature and measured temperature at each point. The program passes the resulting error to the objective function as the value to minimize when using *fminbnd*. Iterations are performed until the program cannot significantly reduce the error, and a final optimized value of diffusivity is returned as output. An optimum is reached when the solver attempts to take a step size to a new diffusivity that is smaller than a specified tolerance, resulting in a converged solution.

An appropriate range for diffusivity was determined by addressing literature for past laboratory studies that evaluated thermal properties of concrete. Although no diffusivity values initially could be found for pervious concrete, one published source listed thermal diffusivities of standard concrete ranging from 0.38 to 2.04 ft^2/day depending on the type of aggregate used (Lamond et al., 2006). During preliminary analysis using the model, it was found that pervious concrete had a diffusivity consistently below 1 ft^2/day. Therefore, a range of 0 to 2 ft^2/day was used to search for diffusivity of the pervious concrete pavement test cells. A range of 0 to 3 ft^2/day was used for the PCC test cell based on the range provided by the referenced source.

3.6 Analysis Intervals

For many reasons discussed below, the decision was made to separate the 4.5 years of data collected for each cell into smaller time increments and analyze individually the thermal diffusivity for each time segment. Given that each sensor collected approximately 155,000 data points over the time interval analyzed, and each cell has at least five sensors in the pavement layer, the computational effort was substantial. The solver would be required to calculate a solution to the partial differential equation at 775,000 point for each iteration of the optimization process if the data required was

analyzed as a whole. It was found that the built-in *pdepe* function itself was a considerably slow solver, even when analyzing significantly small portions of data (a period of one day, for example) and eliminating embedded functions within the full program. When running the optimization program, almost all of the processing time was spent within the actual code of the *pdepe.* Consequently, more efficient coding throughout the rest of the program would have little effect in speeding up the processing time. Moreover, when longer periods of time were analyzed, the computation time was growing exponentially, not linearly, as may be expected. In response, the *DiffuModel* program was written to accept the full data record, a desired time interval (such as one day, one week, or one month), and a specific start date as input. Then a separate function was included in the *DiffuModel* program to segment the data and solve for a fitted diffusivity value for each interval as the output. The program also returned the corresponding calculated error for each fitted thermal diffusivity. This approach allowed for experimentation with different time period lengths for the best mix between accuracy and computing time. It was found that time periods of too short a duration returned highly variable results, as shown in the following chapter. Ultimately, segmenting the data into one-week periods provided optimal results.

This approach was beneficial in many ways. First, it allowed for the evaluation of changes in thermal diffusivity over time. For example, a plot of the time series of the results could be used to determine whether any effects existed from clogging, general deterioration, or maintenance events of the pervious pavements. It could also be used as a way to evaluate any seasonal trends in the data. Additionally, segmenting the data was used a screening tool to help identify possible faulty temperature readings. Although it was infrequent (such as three consecutive faulty readings in one sensor over a span of a couple months), the sensors periodically recorded improbable values that had the potential to disrupt the model and make the optimization process unsuccessful. By segmenting the data, it was possible to isolate the error to a single period of optimization which could later be flagged in the final results without influencing the accuracy of the valid measurements and resulting fitted diffusivities.

3.7 Graphical Output

Among other reasons, graphical output was included as an additional tool to address inconsistent data collection. After initial inspection of the data, it was found that the sensors would periodically time out for consecutive intervals. For the partial differential equation solver to function accurately, it was necessary that the intervals between measurements be consistent. In addition, when data is imported into MATLAB as a variable from the original .xls file format and an entry is blank, the MATLAB's default is to fill the entry with zero versus leaving the cell empty. Because the program could still run with zero values, this was found to significantly affect the boundary conditions and resulting solutions. To account for the missing data, an additional embedded function was added to the *DiffuModel* program to detect gaps, and then perform linear interpolation to produce a continuous data record.

Graphical output was also added as a tool to quickly verify that the interpolation was being completed accurately. The graphical output was also used throughout the program development to correct errors in the optimization process and identify any faulty data. Two options were included: (1) to graph the full solution to the partial differential equation in a three-dimensional mesh plot, or (2) to plot the solution at the middle sensors against the raw data in a two-dimensional plot to evaluate the accuracy of the fit. Examples of this output for a two-day period are given in figures 2 and 3. The generated three-dimensional temperature profile follows the expected behavior: the pavement is warmer at the bottom and cooler at the surface during the nighttime, and warmer at the surface and cooler at the bottom during the daytime. The two-dimensional plot also shows a close fit between the model and actual temperature measurements.

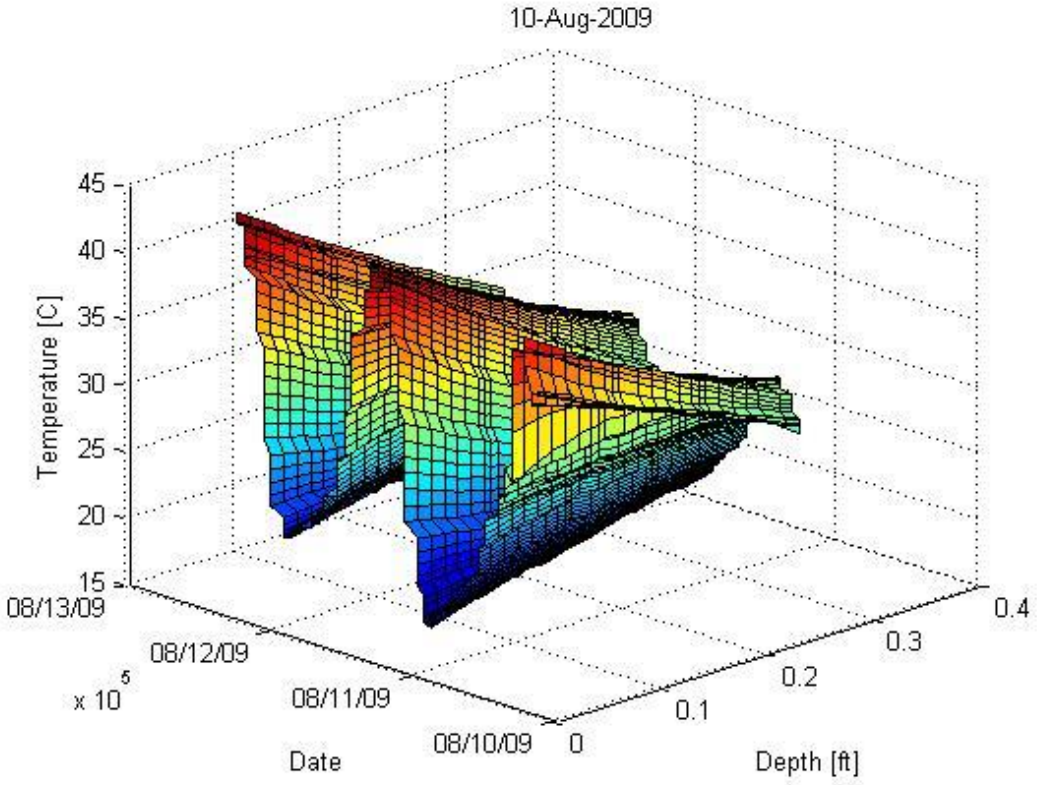

Figure 2: Mesh 3-D Partial Differential Equation

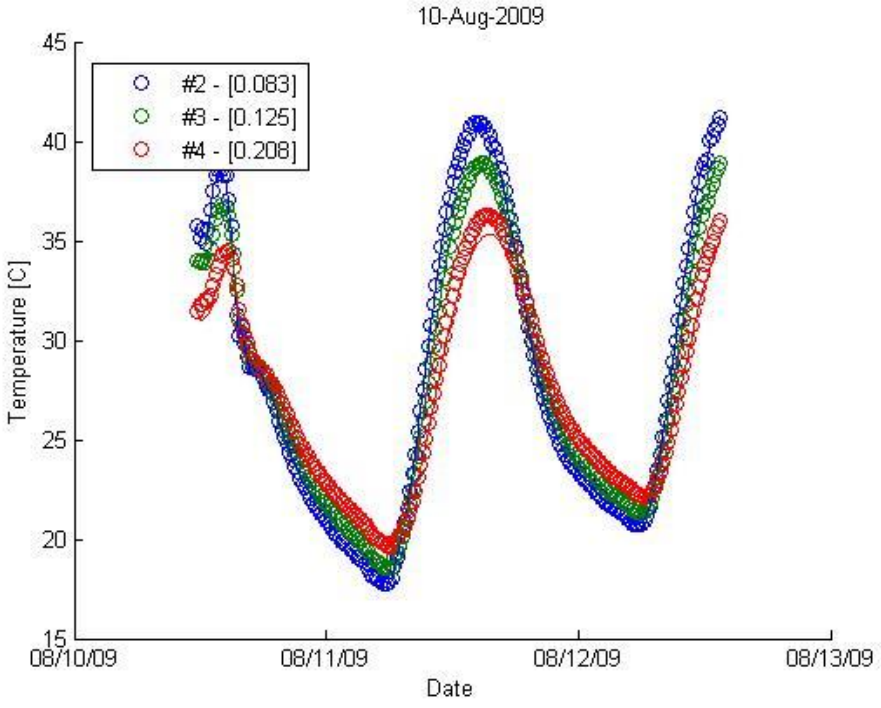

Figure 3: Solution versus Raw Data

CHAPTER 4: THERMAL DIFFUSIVITY RESULTS

4.1 Cell 85

Initial results from the analysis of the thermocouple data from Cell 85 showed that after nine weeks of data, the optimization was continually hitting the bounds of the search. However, results from the first eight weeks were fairly consistent with those found in the other pervious concrete pavement test cells. To investigate this behavior, the raw thermocouple data was plotted and thoroughly inspected. It appeared that the sensors began to give unreliable measurements as the temperatures dropped down to very cold temperatures during the first winter the sensors were in operation.

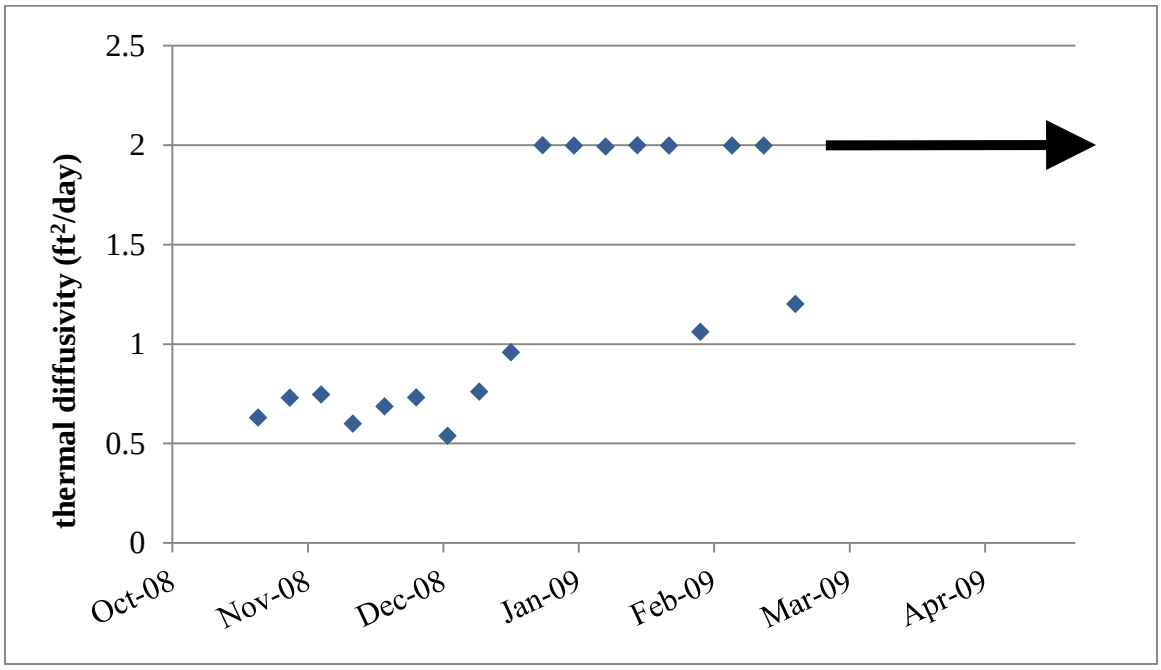

Figure 4: Cell 85 Diffusivity – 1 Week Intervals

In an attempt to salvage the good data which is available during the first couple weeks after installation, as well as evaluate how the diffusivity results would vary when shorter data periods are used for optimization, a one-day period was used in the following analysis.

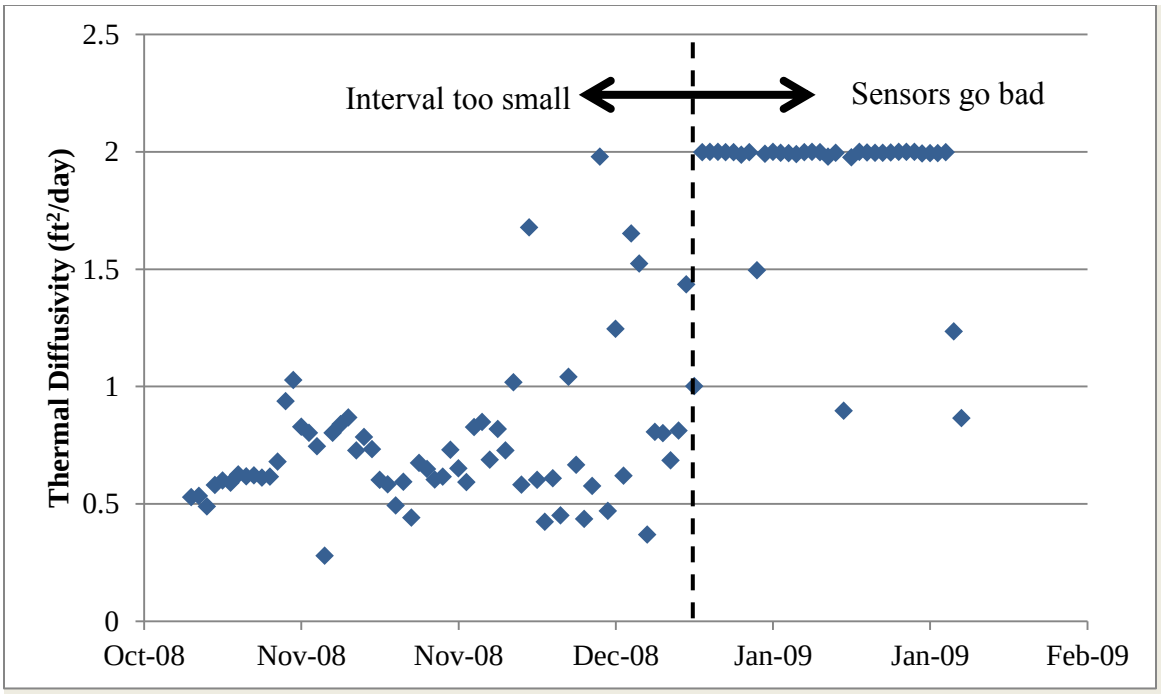

Figure 5: Cell 85 Diffusivity – 1 Day Intervals

Figure 5 clearly shows that with one-day intervals, there is not sufficient data to fit an accurate temperature gradient using the heat equation, and the diffusivity results become highly variable. Therefore, it was determined that daily fluctuations in temperature over multiple days are required to fit an accurate value for diffusivity. Consequently, one week intervals were used in the analysis of the remaining test cells.

4.2 Cell 89

The results in Figure 6 show that the diffusivity hits the bounds of the search only in only four instances over the 4.5-year period analyzed. These four weeks of data were assumed to be a result of faulty recordings by the thermocouple sensors and were eliminated from the analysis. Figure 7 shows that the fitted thermal diffusivity values stay relatively constant, with an expected amount of variability about the mean. Cell 89 has an average diffusivity of 0.61 ft^2/day. There is not a very clear seasonal trend or a change in average diffusivity over time when looking at the graphical results; however, closer inspections found that the diffusivity is generally higher in the winter months than in the summer months, varying inversely with temperature. The minimum fitted diffusivity was 0.497 ft^2/day. A linear trend line of the results up until Fall 2012 shows a slope of nearly zero

(-5E06). However, the slightly negative slope may indicate a minimal reduction in thermal diffusivity of the pervious concrete pavement over time due to changes in the material composition.

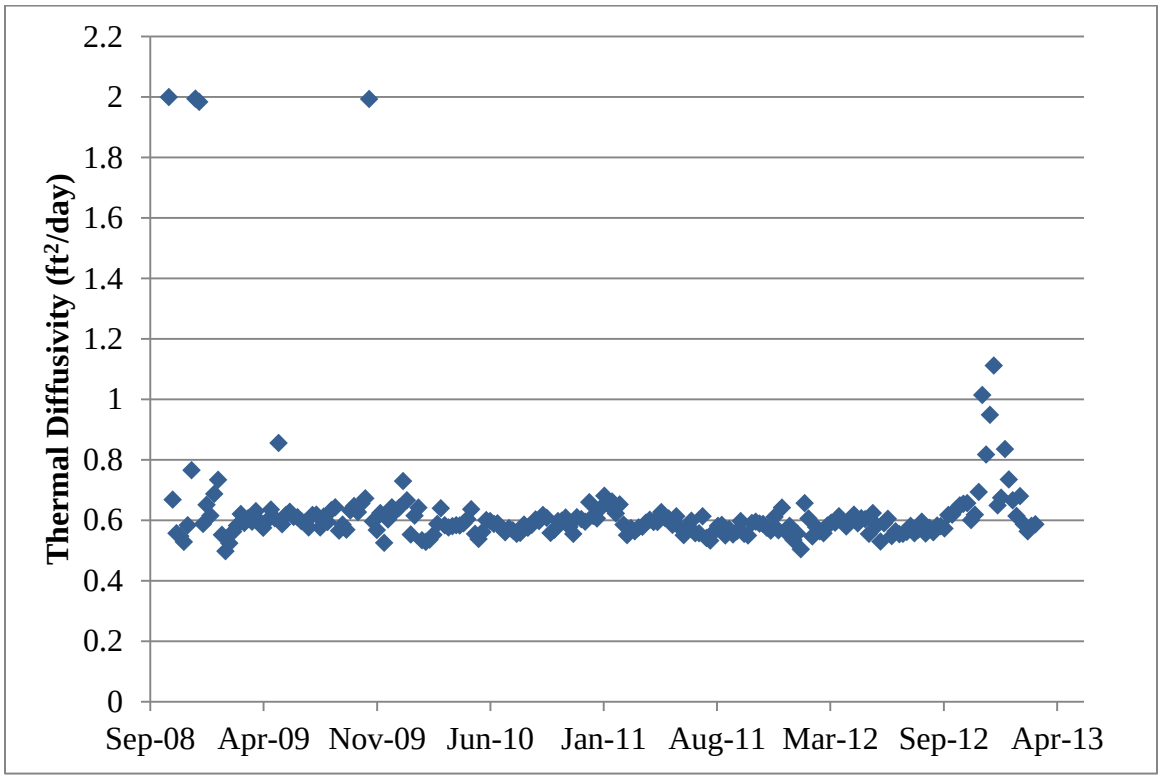

Figure 6: Cell 89 Thermal Diffusivity – All Results

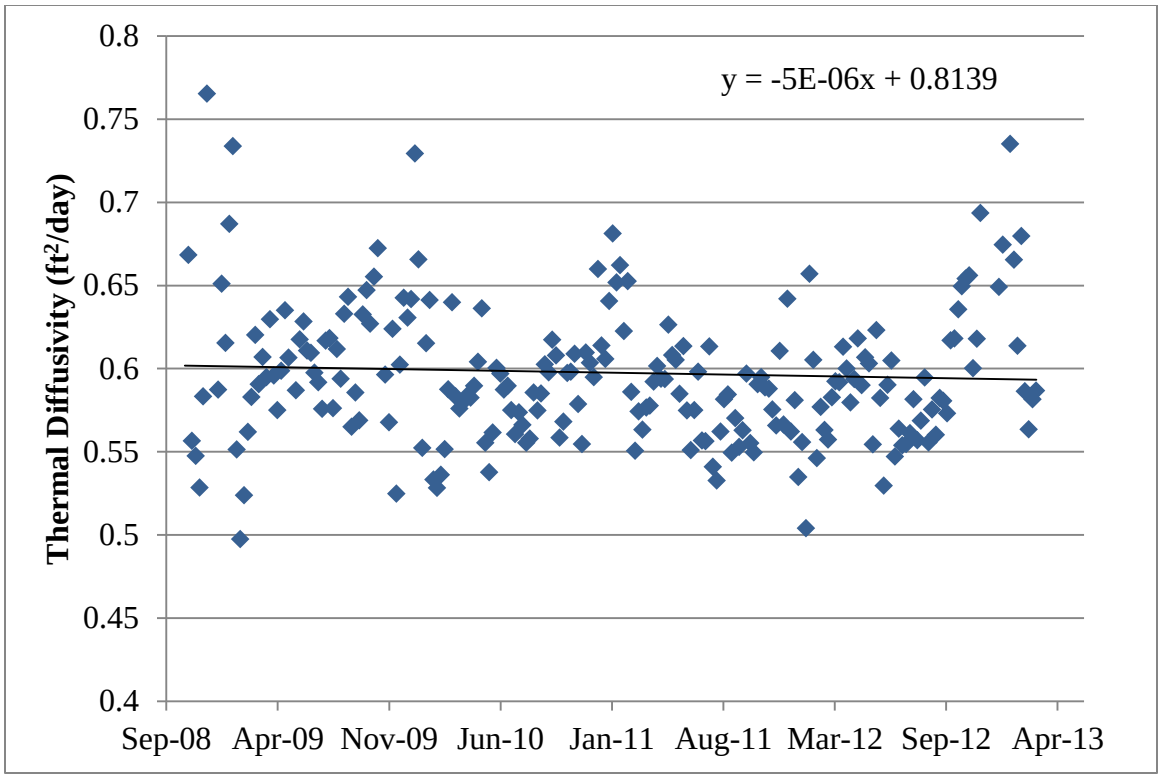

Figure 7: Cell 89 Diffusivity – Good Data

4.3 Cell 39

The results for Cell 39 had much more variability than Cell 89. During the winter of 2009/2010 and 2010/2011, the optimization hit the bounds of the search for a ten-week period. It is possible that the sensors were unable to function correctly in extremely cold winter temperatures. This could also be explained by the fact that there was trapped frozen water filling up the voids of the pervious concrete. For instance, if this water was only present in the bottom of half of the pavement depth, it may only affect two of the five sensors. This may fail the heat equation model, which assumes a continuous homogenous material. Although it is difficult to visualize with the missing data in the winter months, there seems to be seasonality in the results, with diffusivity values in the summer months being lower. When the erroneous results are eliminated, a linear trendline finds a slightly negative slope one order of magnitude larger than what was present in Cell 89. The average diffusivity of Cell 39 is 0.68 ft^2/day.

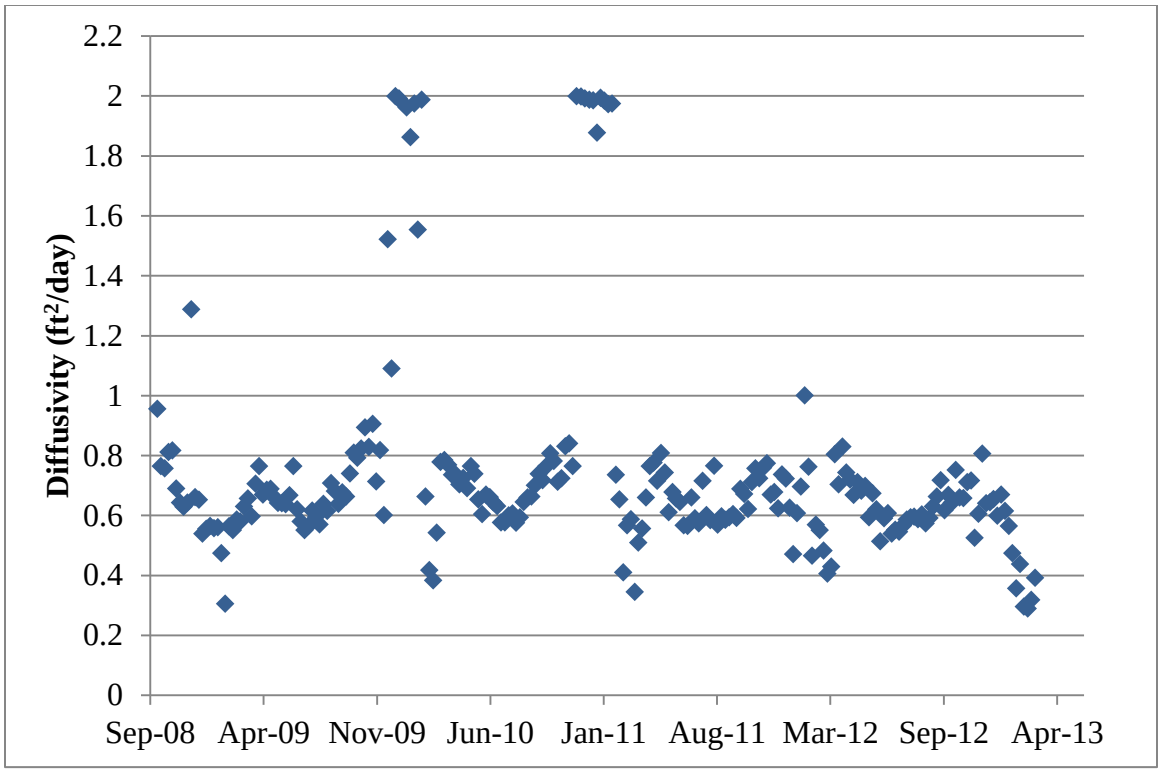

Figure 8: Cell 39 Diffusivity – All Data

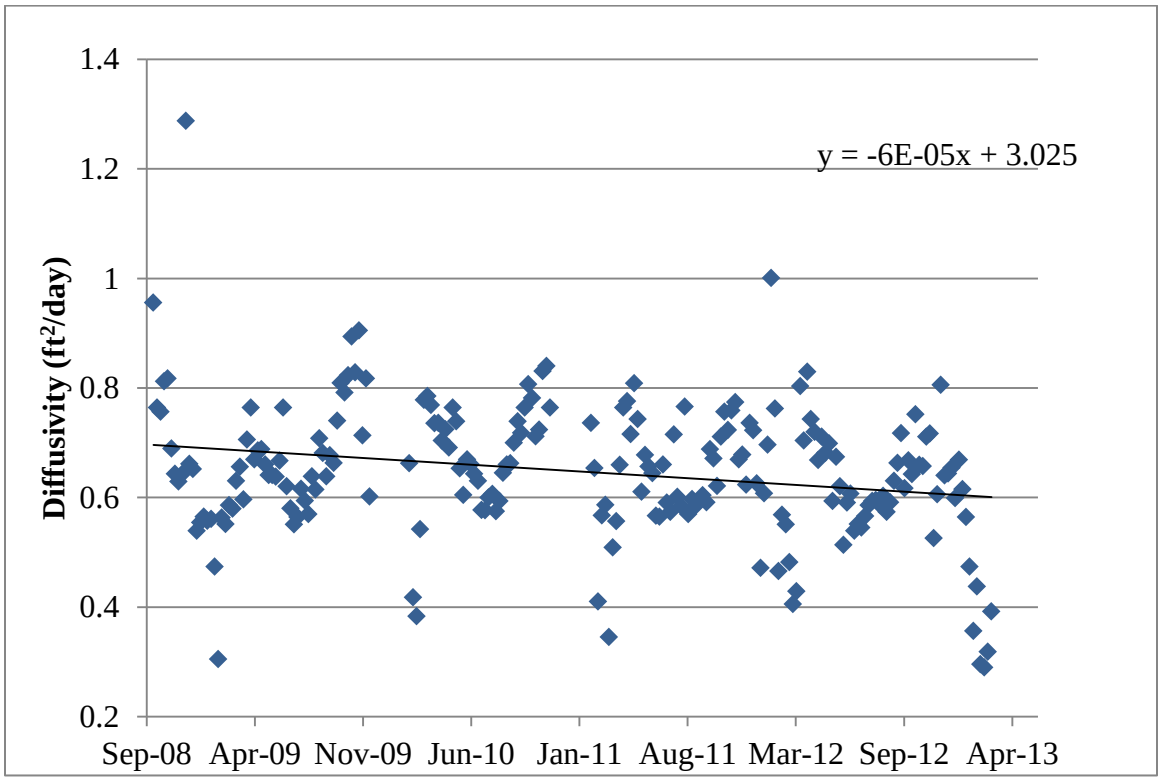

Figure 9: Cell 39 Diffusivity – Good Data

4.4 Cell 64

The diffusivity of Cell 64 was slightly lower than the other pervious test cells analyzed in this research, with an average value of 0.47 ft^2/day. However, it is clear that the data was extremely erratic during the winter months. When the raw data is plotted, the sensors appear to be collecting accurate data. This behavior in the winter may be caused by trapped moisture in the pavement layers, cold temperatures, or large fluctuations in temperature due to precipitation events near the surface of the pavement that could not be accurately modeled by the program The fitted thermal diffusivity in Cell 64 also has a very slight decreasing trend over time. The slightly negative slope of the linear trend line is was in between those found in cells 89 and 39.

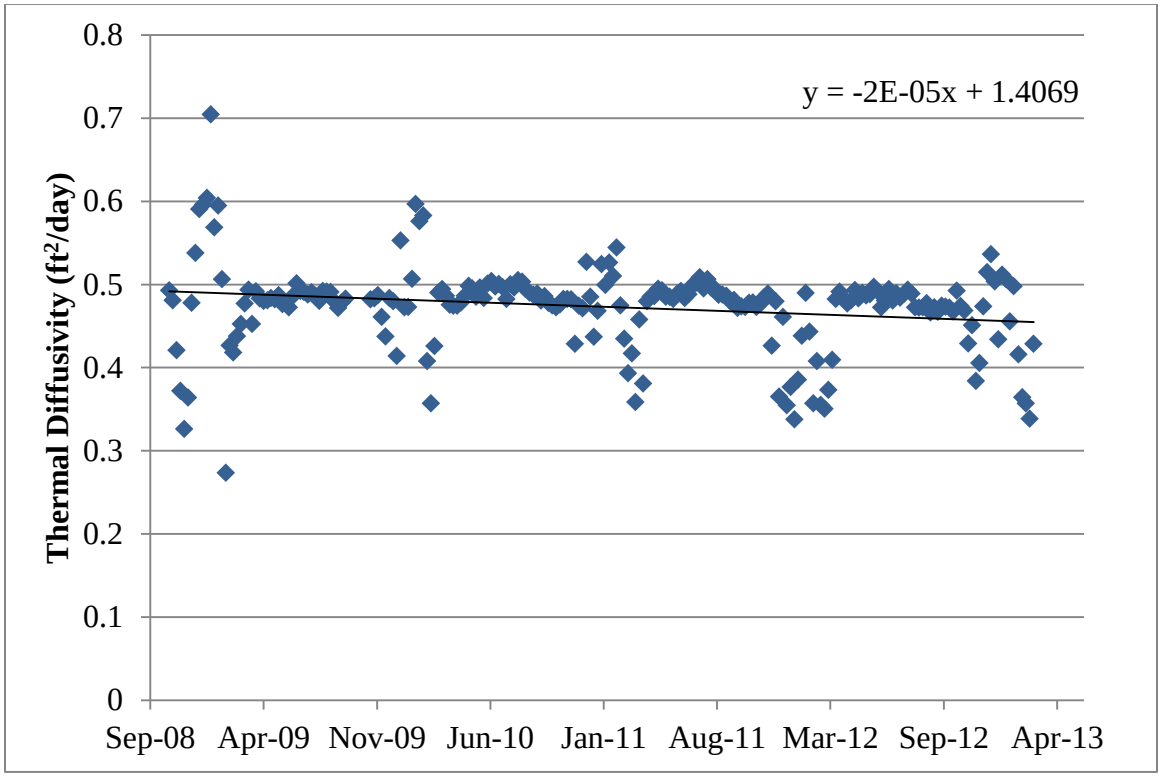

Figure 10: Cell 64 Diffusivity – All Data

4.5 Cell 52

The impervious PCC in Cell 52 had diffusivity values nearly three times that of the pervious test cells analyzed in this research, confirming that pervious concrete does have substantially different thermal properties than typical non-pervious concrete. Results hit

the bounds of the search during only two data periods over the 4.5 years analyzed. When these erroneous data periods were eliminated, the average thermal diffusivity of Cell 64 was 1.73 ft^2/day. This value is consistent with those values found in literature for PCC made with similar aggregates, and helps to validate that the *DiffuModel* program can produce accurate results (Lamond, 2006). Cell 52 has a more noticeable decreasing trend over time compared to the pervious concrete cells, with the slope of the linear trend line being one order of magnitude larger than cells 39 and 64. There are also signs of seasonality in the results, with diffusivity lower in the summer months and higher in the winter months, similar to what was found in some pervious test cells.

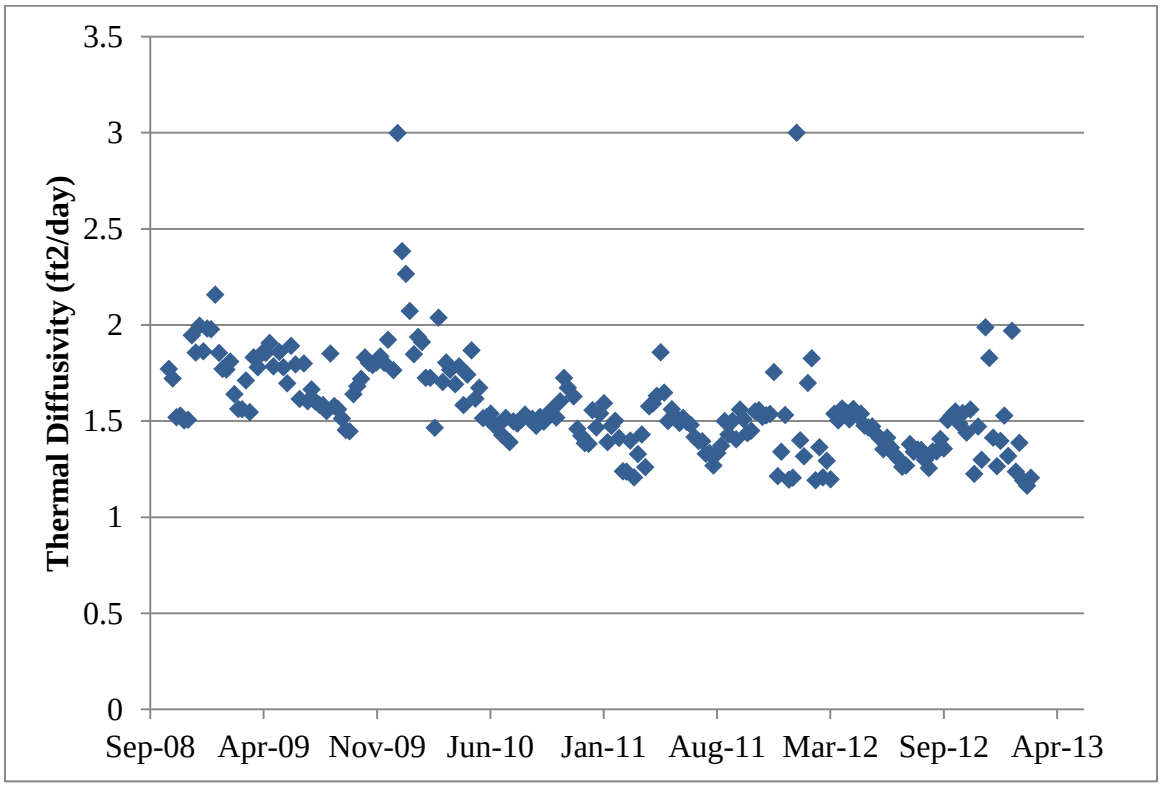

Figure 11: Cell 52 Diffusivity – All Data

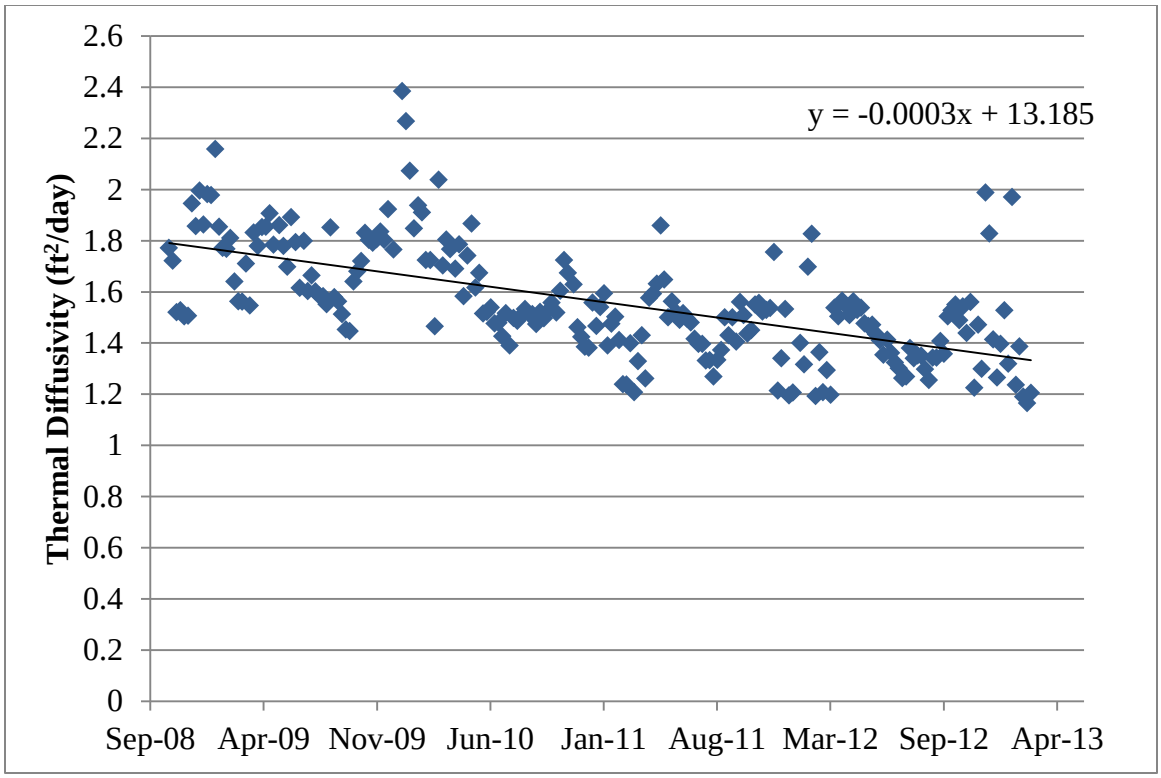

Figure 12: Cell 52 Diffusivity – Good Data

4.6 Diffusivity Summary

The fitted thermal diffusivity results presented in this chapter suggest that pervious concrete has significantly different thermal properties that standard Portland cement concrete when measured from in-situ temperature data. Figure 13 presents the average diffusivity of all cells. The value presented for Cell 85 was taken from the nine weeks of good data. The three pervious concrete pavement test cells in the Low-Volume Road all have very similar diffusivity, around 0.65 ft^2/day. The pervious concrete driveway, Cell 64, has a slightly lower diffusivity, but this may be a result of the highly variable diffusivity results during winter months in this test cell. All concrete diffusivity values showed a decreasing trend over time, which may be due to changes in the air void structure of the concrete with deterioration or clogging of the pavements. Diffusivity of the standard PCC cell is consistent with laboratory tested values and helps to confirm that the *DiffuModel* program can find accurate thermal diffusivities from the thermocouple data.

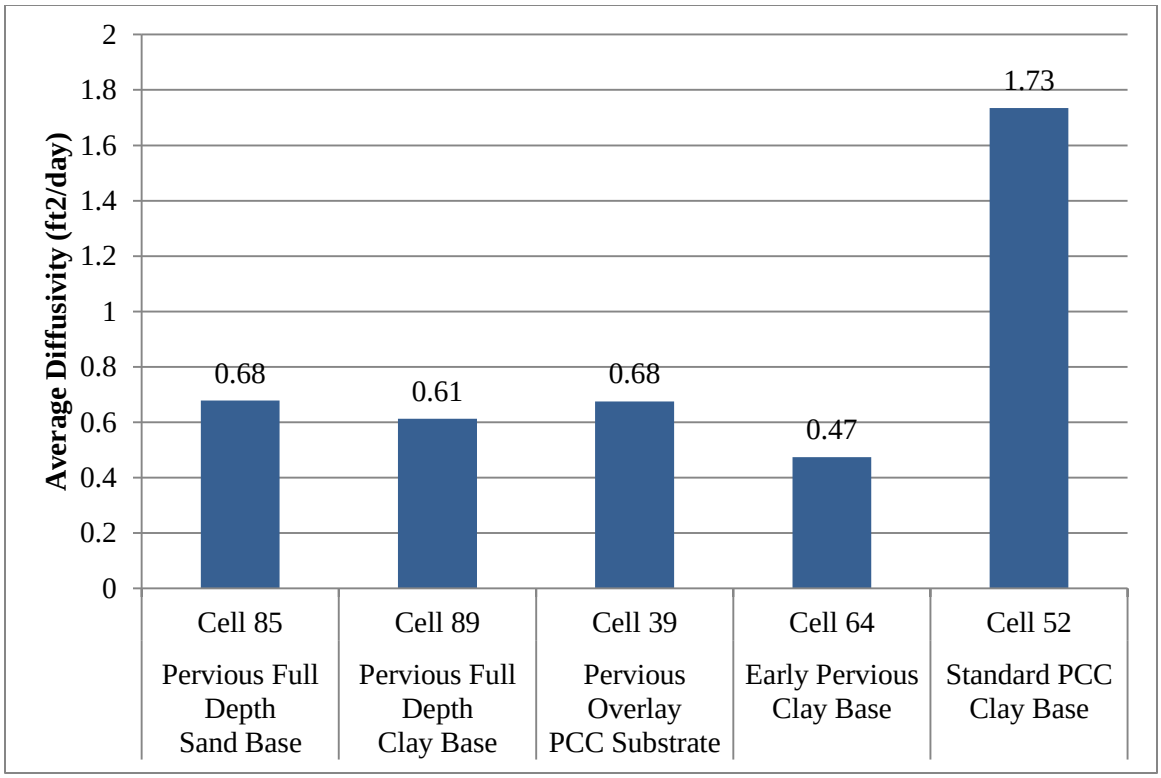

Figure 13: Average Diffusivity – All Cells

CHAPTER 5: VALIDATION OF DIFFUSIVITY MODEL

A second program was written in MATLAB to validate that the *DiffuModel* optimization program was functioning correctly and finding the diffusivity that most closely matched the measured thermocouple data. The program develops a synthetic temperature gradient at the middle sensors given specified boundary conditions (temperatures at outer sensors) and initial conditions (temperature at all sensors at time zero). The synthetic temperature gradient is also dependent on a specified thermal diffusivity which is entered as input to the program. Once a temperature gradient with a known diffusivity has been established, the original MATLAB program was used to test if the optimization process can identify the correct, known, diffusivity.

Three validation runs were performed. One week of data from cell 89 was used for the boundary and initial conditions. The measured temperature data from the top and bottom sensors for the week was entered as boundary conditions, and temperature data at all sensors at time zero was entered as the initial. Real boundary and initial conditions were used to ensure the accuracy of the optimization program for the same interval length and general scale of temperature variations over time and across depth as was used in the actual analysis.

When the full set of real data at all sensors was run through the *DiffuModel* optimization program, a fitted diffusivity of 0.59 ft^2/day was returned. To validate the code, therefore, synthetic temperature gradients with thermal diffusivities of 0.4 ft^2/day, 0.9 ft^2/day and 1.4 ft^2/day were created. These diffusivities were chosen to be relatively close to the actual diffusivity to assess how a small shift in diffusivity would change the temperature gradient model.

The results from this validation run were very promising. Table 1 summarizes the results.

Table 1: Validation Results

Known Diffusivity (ft^2/day)	Fitted Diffusivity (ft^2/day)	Percent Error (%)
0.4	0.399793	0.05
0.9	0.899846	0.02
1.4	1.400102	0.01

From these results, it is clear that the optimization program is able accurately identify diffusivity values of a given temperature gradient. The percent errors, ranging from 0.05 to 0.01, can be considered almost negligible. The three validation runs verify the program is able to successfully calculate thermal diffusivity of a temperature gradient that exactly follows the heat equation theory.

To understand how a shift in diffusivity would affect the resulting temperature gradient at the middle sensors, the solutions to the partial differential heat equation from the three validation runs were plotted for visual representation. In the legend, s2, s3, and s4 refer to the second, third and fourth sensors in the thermocouple tree. From a basic visual comparison of the three temperature profiles plotted in Figure 14 below, it is clear that a shift in diffusivity can create a noticeable difference in gradients at the middle sensors. Although this difference may appear small, it is compounded by the fact that each analysis period contains 2,016 data points (7 days of data × 24 hours a day × 4 measurements per hour × 3 sensors = 2,016 data points). When the error between all these measured and predicted values is considered together in the minimization of the objective function, the fitted diffusivity value becomes a reasonably accurate estimate.

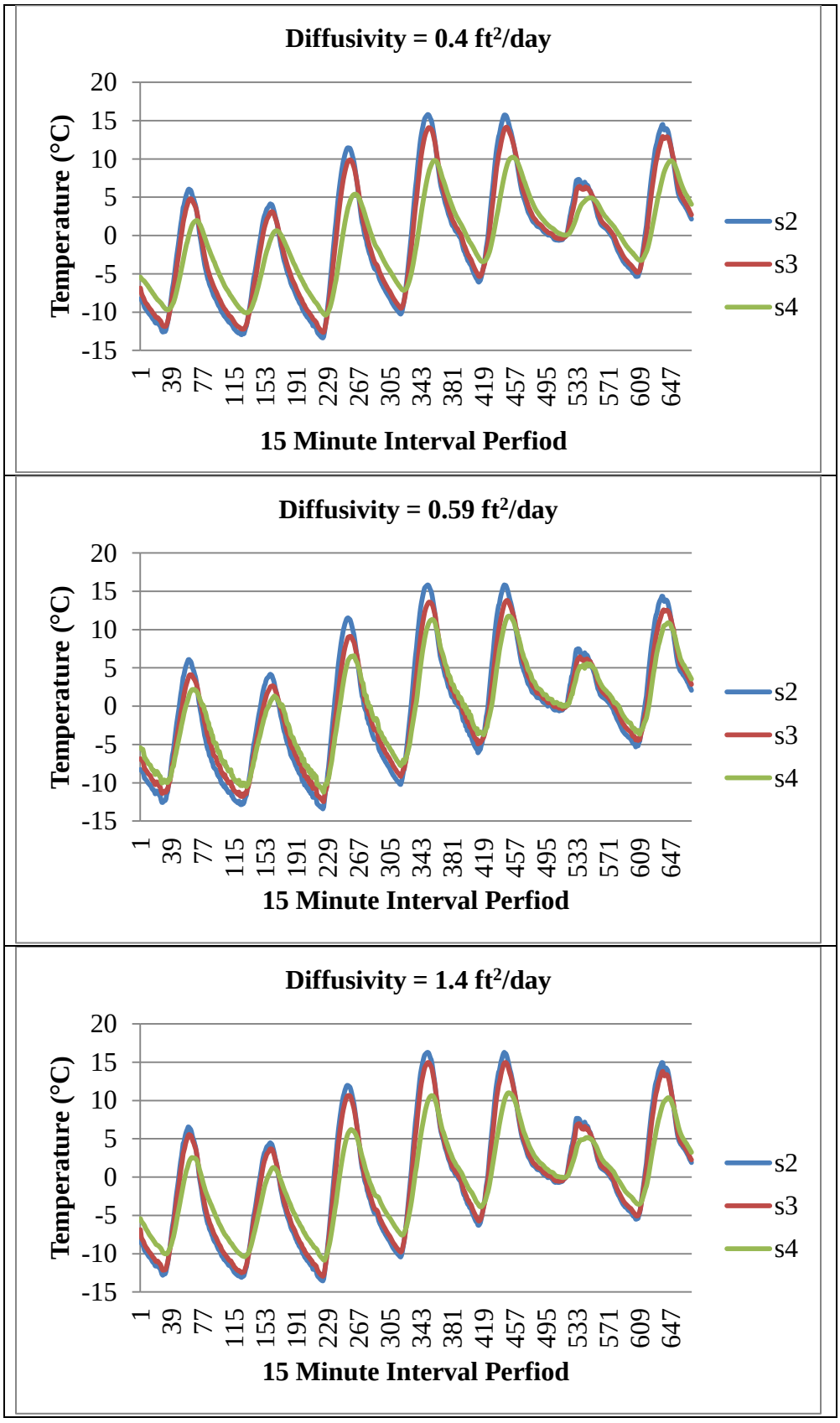

Figure 14: Model Validation

CHAPTER 6: UNCERTAINTY ANALYSIS

6.1 Uncertainty Theory

An uncertainty analysis was performed in attempt to quantify the accuracy of the fitted diffusivity values. This analysis included two calculations: (1) the standard deviation of the error between the measured and predicted values, and (2) the standard deviation of the fitted diffusivity parameter itself. Both of these statistical properties are a measure of the goodness of fit of the model to the data. The calculations were performed for each individual interval over which diffusivity was calculated. This method allows for identification of any trends in the accuracy of the model during certain seasons or over time.

To derive the standard deviations described above, the following definitions are made.

The data consists of temperature measurements from m sensors taken at n distinct times. These measurements are denoted by t_j:

$$\{t_j \mid j = 1, 2, \dots, n\}$$

Therefore, the set of temperature measurements can be denoted by $T_{i,j}$.

$$\{T_{i,j} \mid i = 1,2, \dots, m \; and \; j = 1,2, \dots, n\}$$

The model computes the temperatures at the m locations and n times as a function of a single parameter, diffusivity, defined as α. The model is denoted by $T^*_{i,j}$.

$$T^*_{i,j} = f(i, t_j; \alpha^*)$$

In this model,

- $T^*_{i,j}$ are the true temperatures for all $i = 1,2, \dots m$ and $j = 1,2, \dots, n$, and
- α^* is the true diffusivity.

The associated model for the measured temperature values is then

$$T_{i,j} = f(i, t_j; \alpha^*) + \epsilon_{i,j}$$

In this model,

- $T_{i,j}$ are the measured temperatures for all $i = 1,2, \dots m$ and $j = 1,2, \dots, n,$ and
- α^* is again the true diffusivity, and
- $\epsilon_{i,j}$ are independent, identically distributed, random noise with

$$E(\epsilon_{i,j}) = 0$$

$$Var(\epsilon_{i,j}) = \sigma_\epsilon^2$$

for all $i = 1,2, \dots m$ and $j = 1,2, \dots, n.$

With the given data, the true diffusivity and the true temperatures are unknown. The diffusivity is estimated using measured temperatures by minimizing the sum of the squared modeling errors. The least squares optimal estimate for the parameter is then denoted by $\hat{\alpha}$. Therefore, the measured temperatures can be written as

$$T_{i,j} = f(i, t_j; \hat{\alpha}) + e_{i,j}$$

where

- $\hat{\alpha}$ is the fitted alpha, and
- $e_{i,j}$ are the associated modeling errors for all $i = 1,2, \dots m$ and $j = 1,2, \dots, n.$

Finally, the variance of the error can be estimated using the following formula.

$$\sigma_\epsilon^2 \approx \frac{\sum_{i=1}^{m} \sum_{j=1}^{n} e_{i,j}^2}{mn - 1}$$

Furthermore, the variance of the estimated alpha is approximated by the following formula.

$$Var(\hat{\alpha}) \approx \frac{\sigma_\epsilon^2}{\sum_{i=1}^{m} \sum_{j=1}^{n} \left(\frac{\partial f}{\partial \alpha} \Big|_{i,j,\hat{\alpha}} \right)^2}$$

The partial derivative term may be quickly estimated numerically by the following formula:

$$\left.\frac{\partial f}{\partial \alpha}\right|_{i,j,\hat{\alpha}} \approx \frac{f(i,t_j,\hat{\alpha}+\Delta)-f(i,t_j,\hat{\alpha}-\Delta)}{2\Delta}$$

The partial derivative term is estimated by choosing Δ as a very small number compared to $\hat{\alpha}$. This result follows using a truncated Taylor Series expansion at the point of the optimal fit. The partial derivate term is essentially calculating the change in the solution due to a very small shift in alpha. The standard deviation of each parameter is then calculated by taking the square root of the variance.

6.2 Uncertainty Results

A third program was written in MATLAB that accepts all of the previously fitted diffusivities and the raw data for each test cell, and returns the calculated variance of the errors and variance of diffusivity for each analysis period based on the derived expressions in section 6.1. A value of 1E-04 (0.0001) ft^2/day for Δ was entered into the program, which was appropriate given the small order of magnitude of the diffusivity values. The results provided many notable findings, and are presented in Figure 15 through Figure 22 below.

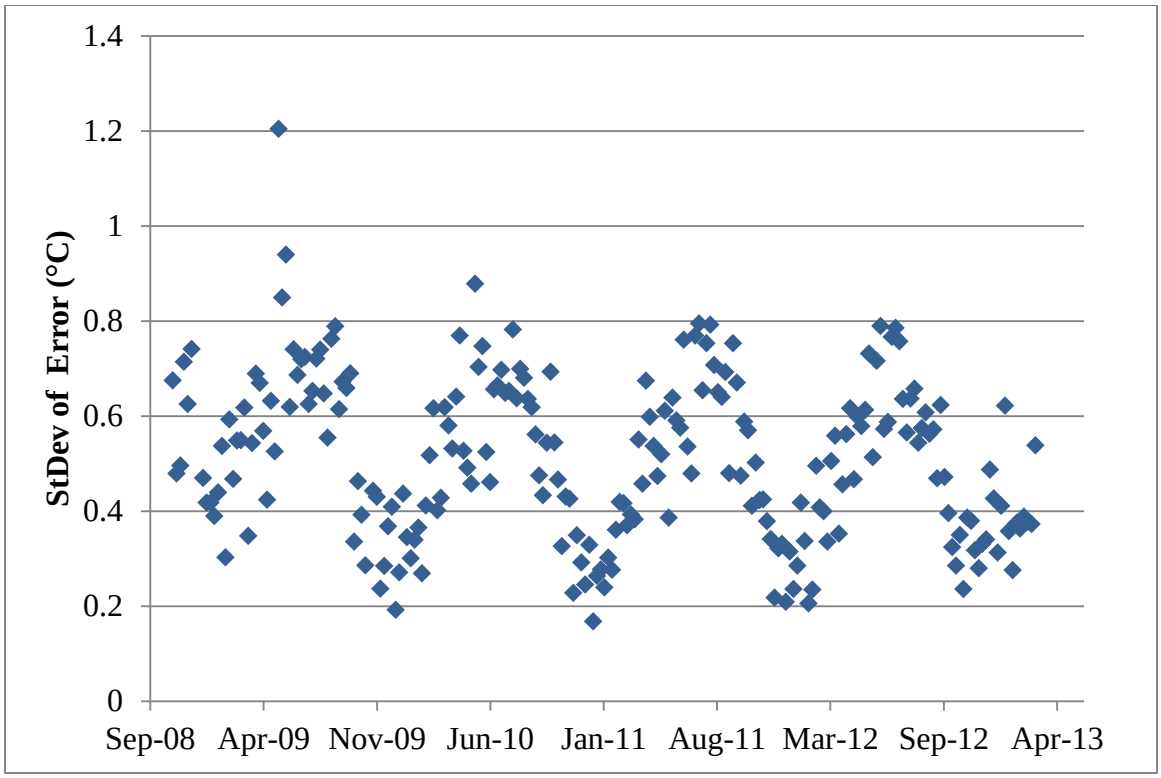

Figure 15: Standard Deviation of Errors – Cell 89

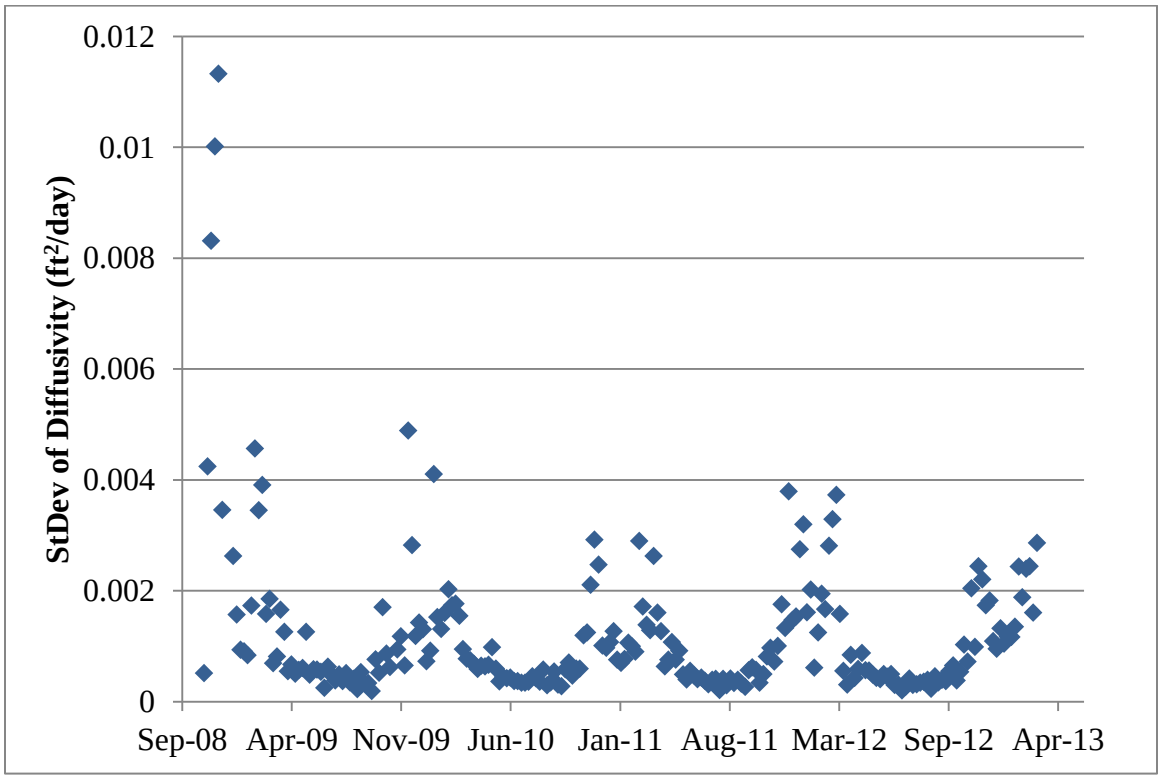

Figure 16: Standard Deviation of Diffusivity – Cell 89

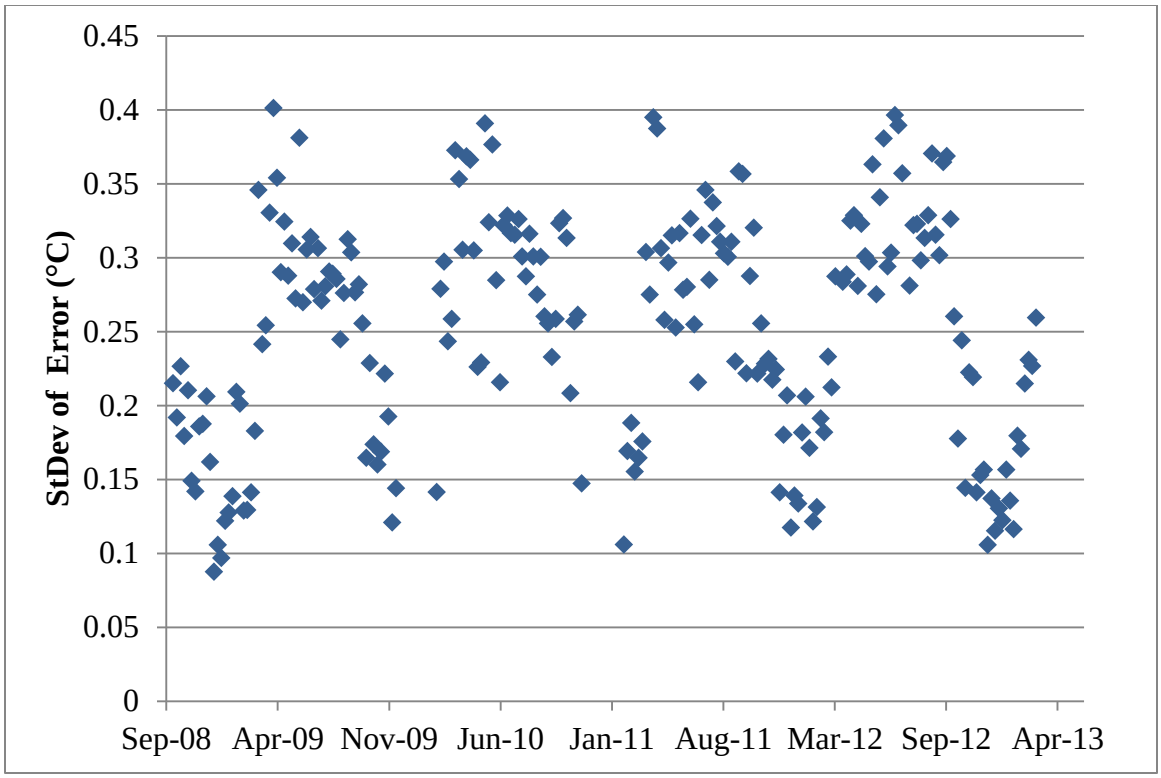

Figure 17: Standard Deviation of Errors – Cell 39

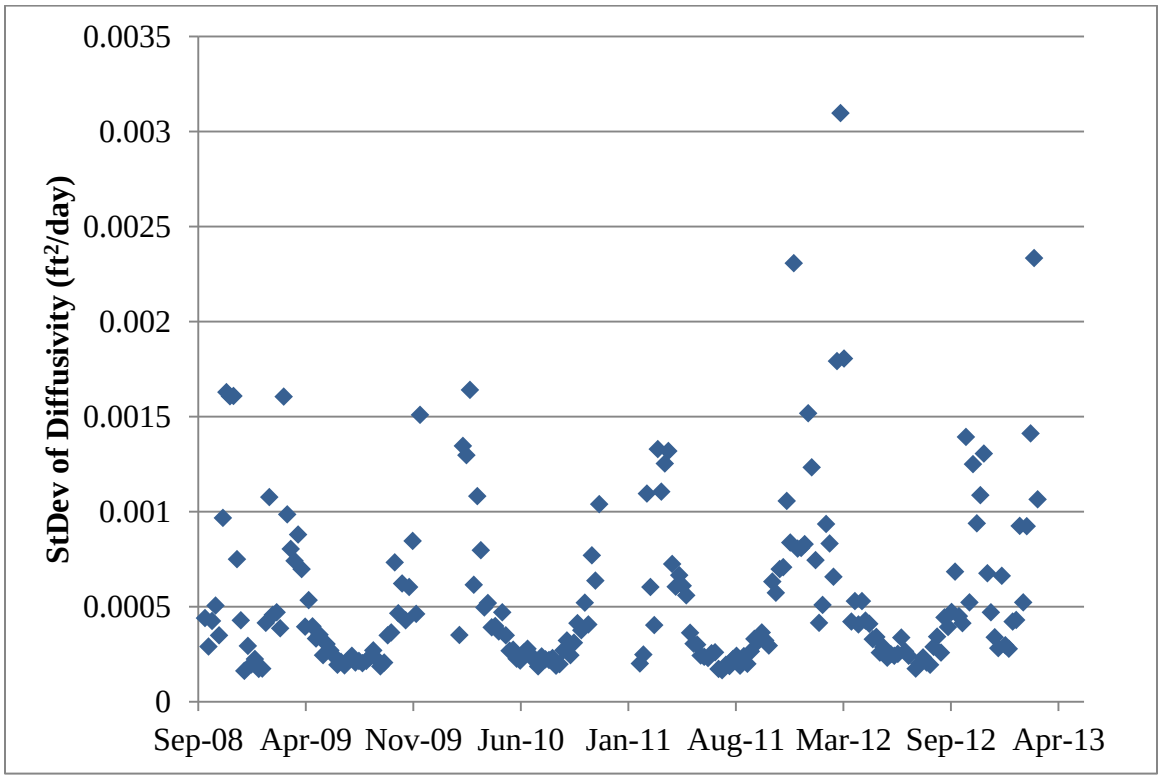

Figure 18: Standard Deviation of Diffusivity – Cell 39

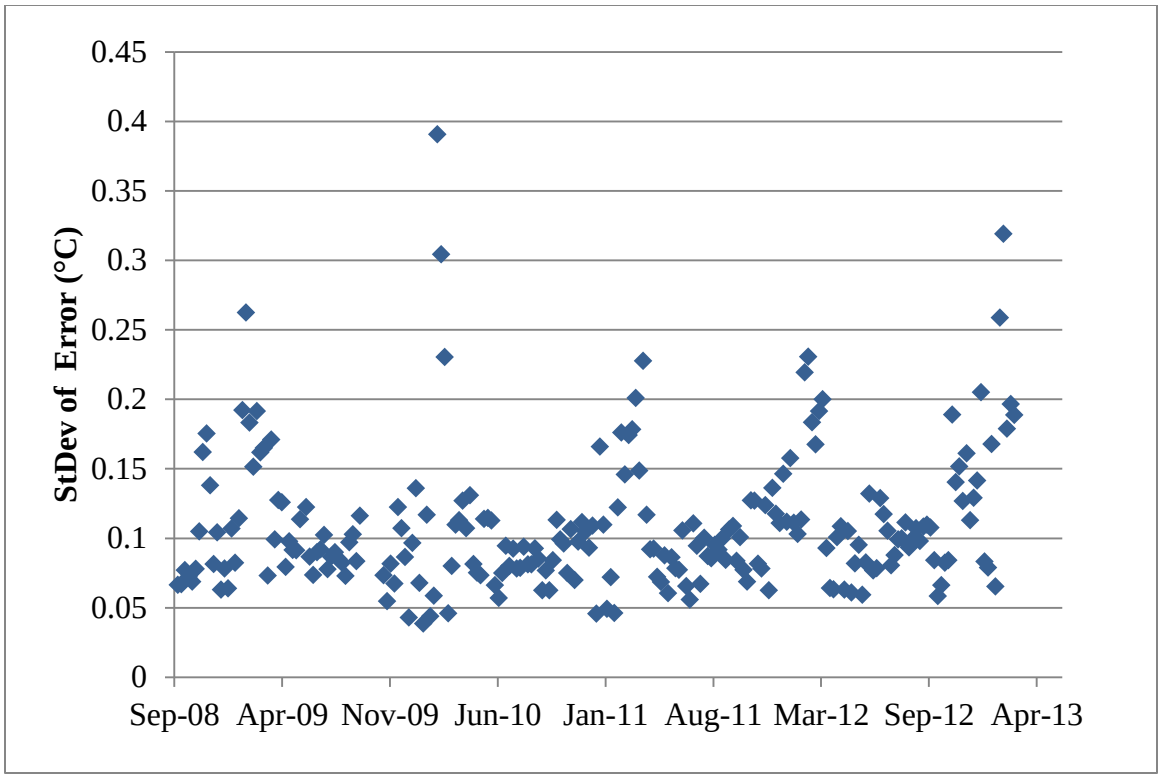

Figure 19: Standard Deviation of Errors – Cell 64

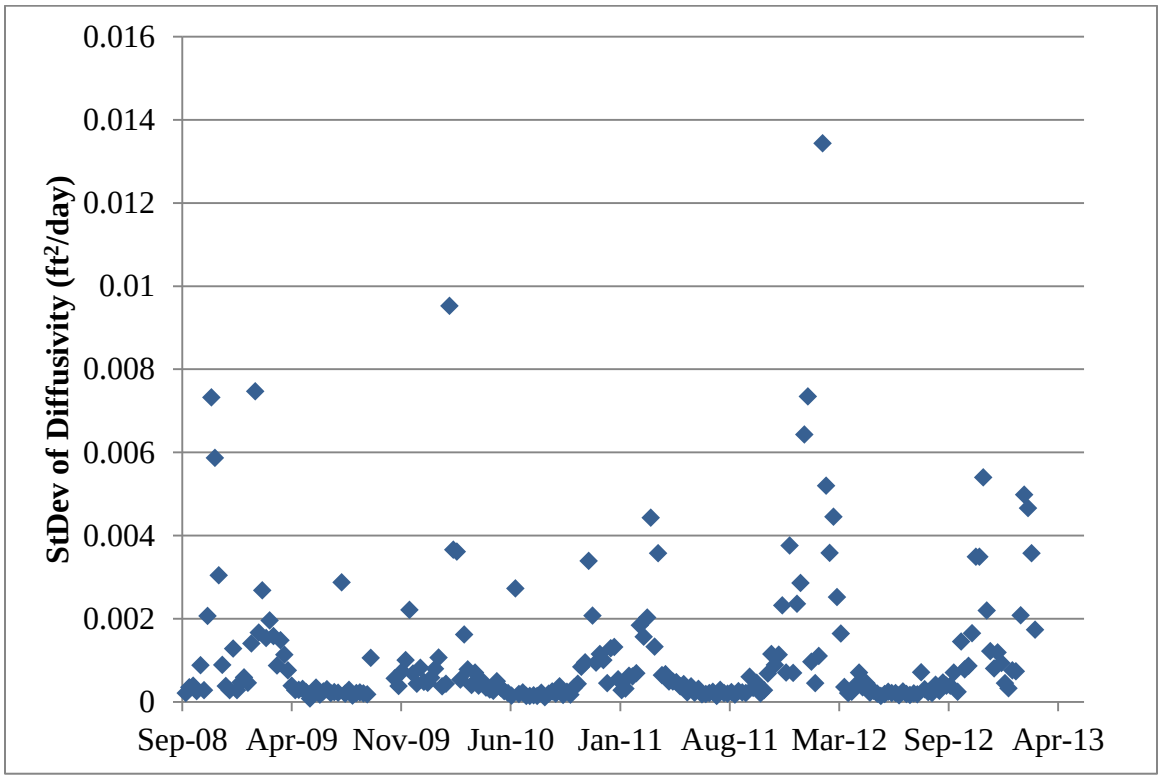

Figure 20: Standard Deviation of Diffusivity – Cell 64

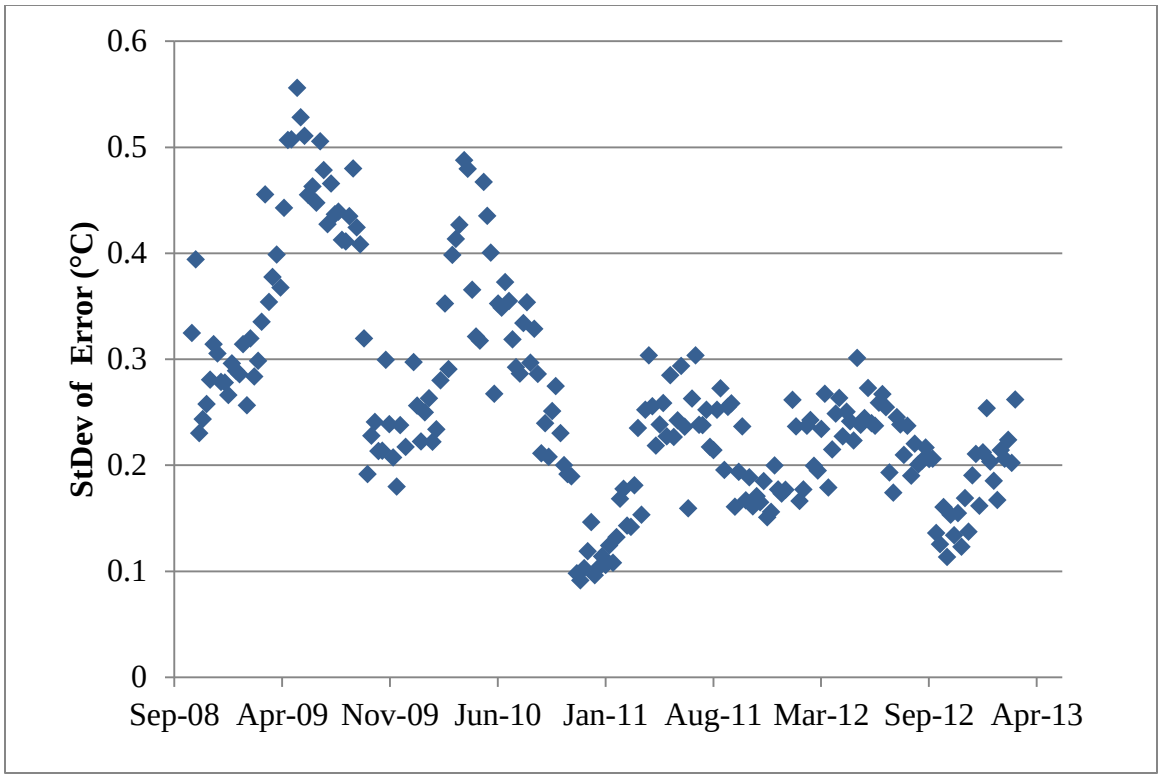

Figure 21: Standard Deviation of Errors – Cell 52

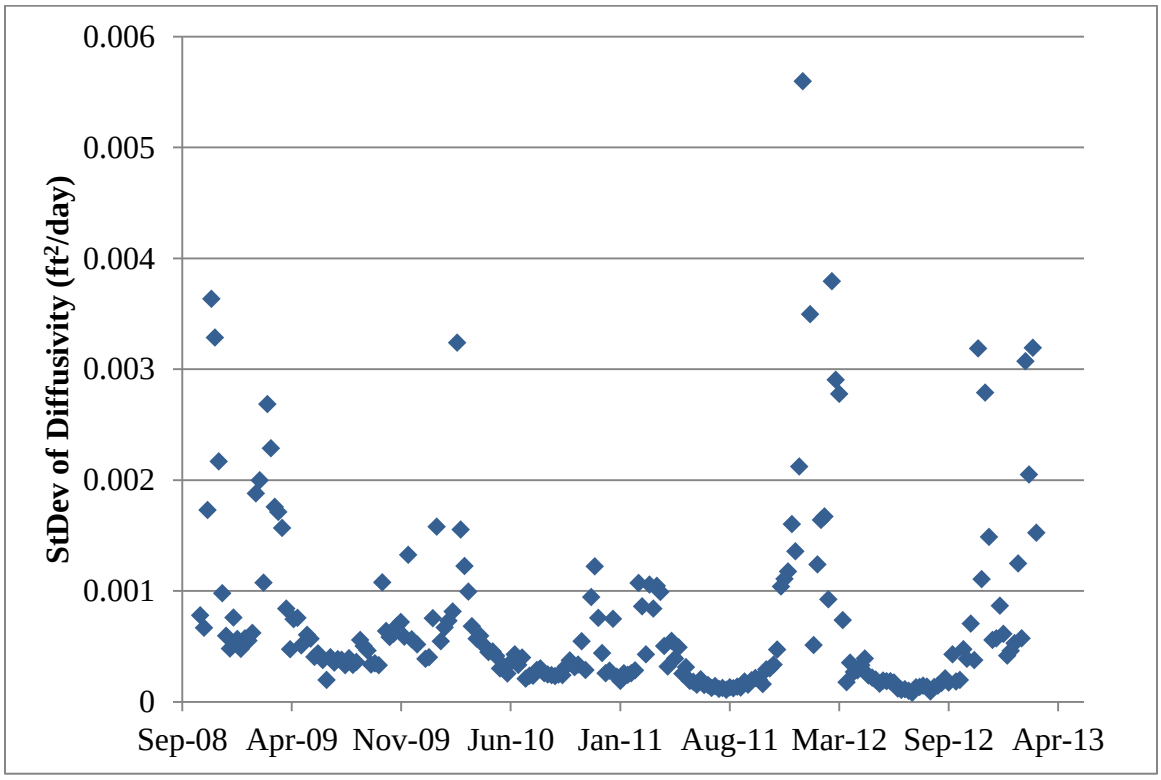

Figure 22: Standard Deviation of Diffusivity – Cell 52

Two significant observations can be made from the results plotted above. Firstly, the standard deviation of diffusivity and the standard deviation of the errors were both considerably low. This is an indication that the modeled temperature values are very close to the measured temperature values at the middle sensors. The low standard deviation of diffusivity also suggests that a slight shift in diffusivity would significantly change the solution, making the estimated diffusivity values more accurate and significant. Both calculated standard deviations were of the same order of magnitude for the three pervious test cells as well and the standard PCC cell. This helps confirm that the values are being calculated correctly in the program and that these small values are appropriate for the large data set being analyzed (over 2,000 test points per interval). The confidence intervals were calculated for the fitted diffusivities assuming a normal distribution. The small standard deviations and extremely large data set results in intervals of around 0.01% on either side of the fitted diffusivities for a 99% confidence level

Secondly, there is a very drastic seasonal variation in the standard deviation) of errors, as well as in the standard deviation of diffusivity. The seasonal fluctuations in the standard deviation of errors smoothly increases and decreases across seasons. However, the standard deviation of diffusivity seems to spike in the winter months. Most importantly, the seasonal fluctuations between these two properties are opposite. In the summer months, the standard deviation of errors is high and the standard deviation of diffusivity is low. In winter months, the standard deviation of errors is low and the standard deviation of diffusivity is high.

6.3 Uncertainty Validation

To explain the opposite seasonal trend between standard deviation of the errors and standard deviation of diffusivity, the equation used to calculate the variance of diffusivity is assessed. To outweigh the effect of a large variance of errors in the summer months, the partial derivative term must be significantly larger in comparison to achieve a low variance in alpha. Conversely, in the winter months, to achieve a high variance in alpha

with a low variance in errors, the partial derivative term in the denominator must be considerably smaller to counteract the low numerator.

To test this theory, one week of data from Cell 89 was chosen from the summer, and one week was chosen from the winter. For each of these weeks, the optimal diffusivity was found and then shifted up by one standard deviation. The new solution to the model at the middle sensors was calculated at each of these shifted diffusivities. Then, the difference between the shifted solution and optimal was plotted for visual representation, where each different colored series represents the difference in the solution at a particular sensor depth.

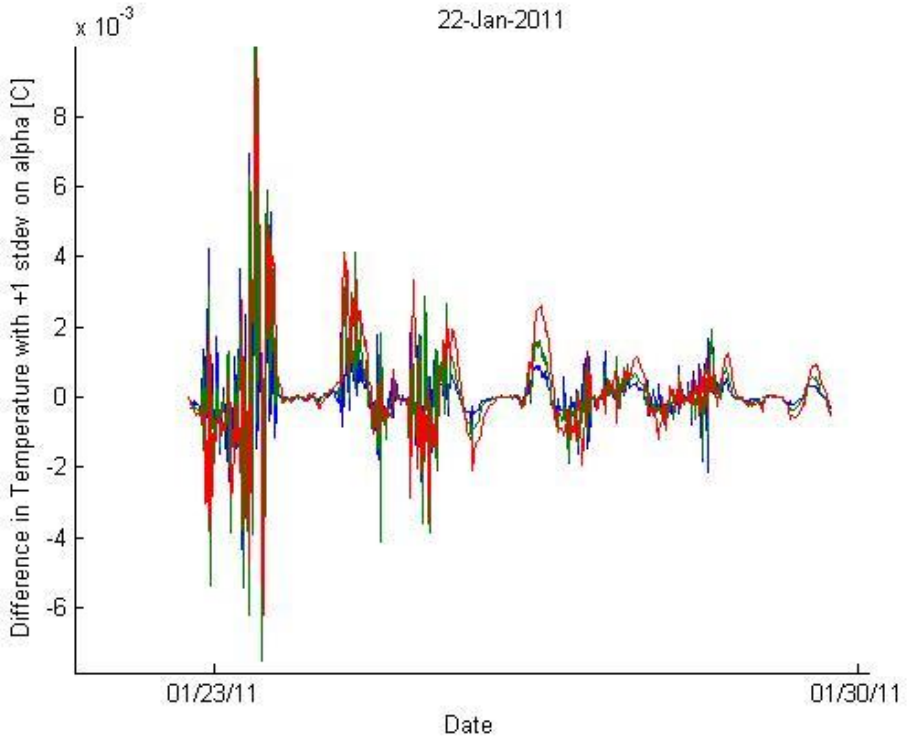

Figure 23: Difference in Solution for Small Change in Diffusivity - Winter

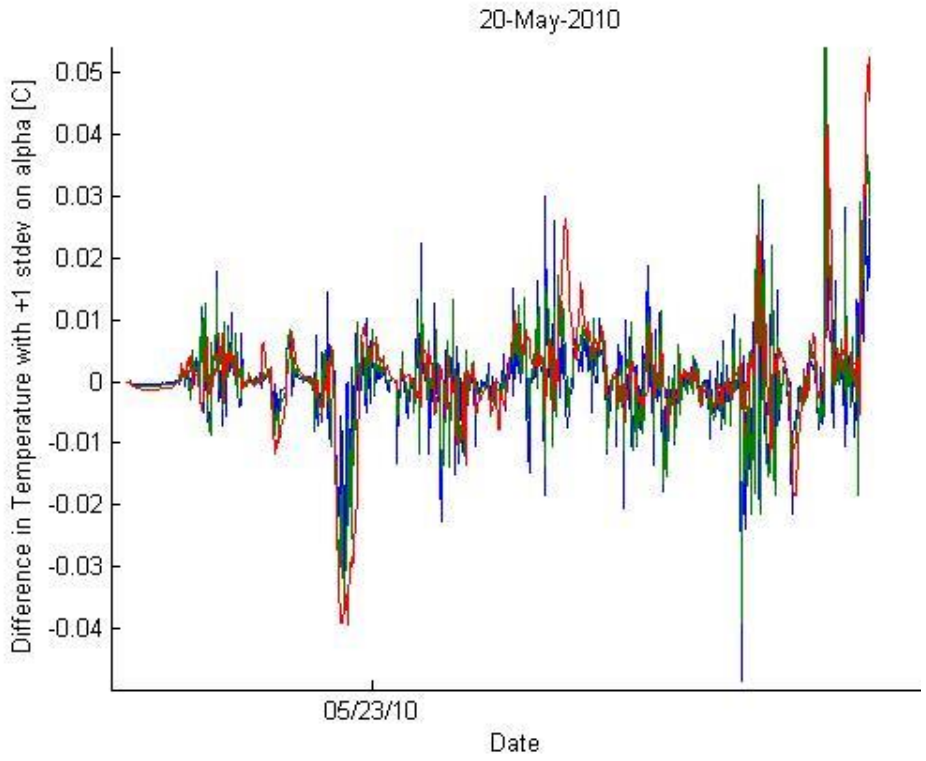

Figure 24: Difference in Solution for Small Change in Diffusivity - Summer

Note that the scale on the winter graph is much smaller than that on the summer graph. The average absolute value of the differences was calculated for each week, with an average in the summer of 0.0051 °C, and an average in the winter of 0.0007 °C. Now, when the partial differential term is considered, where all the differences are squared and then summed, the difference in the denominator between winter and summer becomes substantially more drastic. These results justify the opposing seasonal trends between standard deviations of error and standard deviations of diffusivity.

The change in the root mean squared error as diffusivity was shifted away from the optimal solution was also evaluated. It was found that in the winter, the RMSE does not increase as much as it does in the winter. This suggests that the optimum is more restricted in the summer than in the winter. A possible explanation for these trends is that in the summer months, the data has more variability. The ambient temperature and, consequently, the pavement temperatures, fluctuate more between day and night, making the solution more dependent on diffusivity. These large temperature swings in the

summer will make the boundary conditions highly variable. In turn, a small change in diffusivity will change the solution more drastically than in winter. The best fit solution is more dependent on diffusivity in the summer than in the winter.

CHAPTER 7: COUNTING FREEZE-THAW CYCLES

To further understand the thermal behavior of pervious concrete pavements in contrast to typical impervious Portland cement concrete pavements, an investigation of the freeze-thaw cycles was performed. A 2009 MnDOT study found that the pervious concrete driveway, Cell 64, experienced a reduced number of freeze-thaw cycles when compared to typical PCC pavements of similar thickness [2]. However, the study only evaluated thermocouple and watermark (moisture) data from the winters of 2005/2006, 2007/2008 and 2008 through December 17 and not the more current data analyzed in this research.

Two methods for counting the number of freeze-thaw cycles in the pavement using thermocouple data were presented in the 2009 study:

1. 0°C Method: Counting every fluctuation above and back below 0°C as one cycle
2. Max/Min Method: Counting every time the daily maximum and daily minimum temperature fluctuates above and below 0°C as one cycle.

These two methods were used to test the theory that pervious concrete pavements will experience fewer freeze-thaw cycles than comparable thickness impervious concrete pavements. The analysis was performed on the thermocouple data from the three pervious concrete pavement test cells that had reliable data throughout the 4.5-year period (cells 39, 64, and 89) as well as the standard PCC test cell previously analyzed in this research.

Since the raw thermocouple data is stored in an organized database format, the first method can be completed using Microsoft Excel software and "IF" logical statements to determine every time the temperature at a particular sensor crosses above and back below a temperature of 0°C. A worksheet template was created where portions of different thermocouple database tables from each cell could be entered in the spreadsheet, and the total number of freeze-thaw cycles at each sensor would be automatically calculated for that particular time period. Using this spreadsheet, the total number of freeze-thaw cycles was calculated at each sensor in each cell throughout the four-and-one-half winter seasons from fall of 2008 to early spring of 2013.

In the first iteration of the 0°C Method for determining for determining freeze-thaw cycles, the results showed an unrealistically large number of freeze-thaw cycles occurring in all of the test cells. This was expected to be caused by temperatures fluctuating very closely around 0°C multiple times for each occurrence of freezing or thawing. With this method, as the phase change is occurring and the sensors are collecting data every fifteen minutes very close to 0°C, there could be multiple "freeze-thaw" cycles defined within a given hour.

As this method was not accurately counting a single freeze or thaw occurring in the material, the spreadsheet was reconstructed to filter the data into either the first, second, third or fourth quarter-hour temperature measurements. Then each fluctuation above/below 0°C was counted for each set of one-hour interval temperature measurements. Finally, the average of each of the first, second, third or fourth quarter-hour freeze-thaw cycle counts was taken as the final number of freeze-thaw cycles for the test cell. The results from the modified 0°C Method are shown in Figure 25 below.

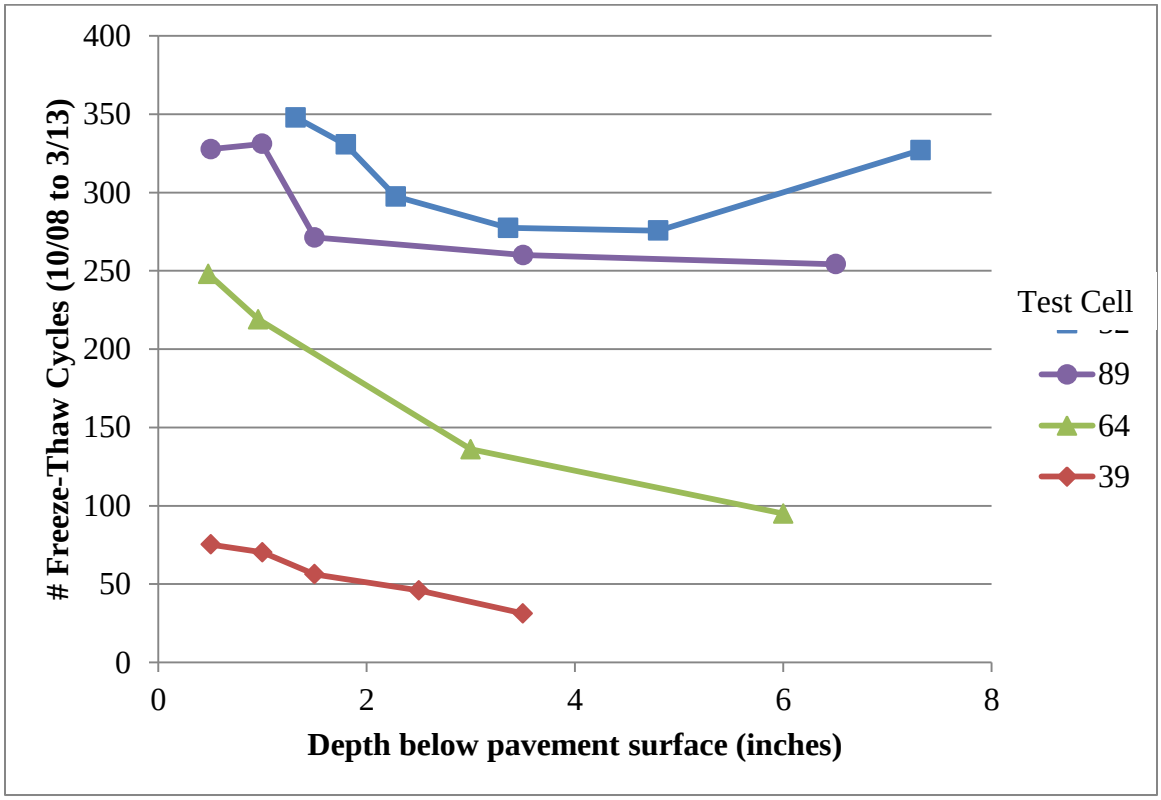

Figure 25: 0°C Method for Counting Freeze Thaw Cycles

According to this method, both the PCC pavement in Cell 52 and pervious concrete pavement in Cell 89 experienced around 50 to 70 freeze-thaw cycles per winter season throughout the pavement depth. The PCC pavement (Cell 52) experienced a slightly higher number total of freeze-thaw cycles than the comparable depth pervious concrete pavement test (Cell 89) at all depths. Consistent with the results found in the 2009 MnDOT study, the pervious driveway clearly experienced a reduced number of freeze-thaw cycles compared to the PCC pavement test cell at all depths. Cell 64 also had a more significant decreasing trend in the number of freeze thaw cycles with increasing pavement depth compared to the other full depth cells analyzed. The average number of cycles per year in Cell 64 ranged from 50 per year at 0.5" depth to only 19 per year at 6" depth. Interestingly, the pervious overlay in Cell 39 experienced very minimal number of freeze-thaw cycles compared to the other test cells analyzed. However, this cannot be used to draw conclusions about the benefits of pervious concrete related to freeze-thaw as the design and thickness of the test cell is much different than the others. The presence of the concrete substrate directly beneath the overlay may also play a part in the reduced number of cycles detected. It may be possible that once the overlay material becomes frozen it stays frozen longer; alternatively, it may freeze earlier in the season and consequently may not undergo as many intermediate cycles before the coldest months of winter.

Next, to perform the Max/Min method for counting freeze-thaw cycles, a program was written in MATLAB that accepts the full thermocouple data record, start date, and end date and computes the total number of freeze-thaw cycles at each sensor depth for that time period. To reduce processing time, a MATLAB script was also written to automatically compute the total freeze-thaw cycles across all 4.5 winter seasons as well as for each season separately for each cell. The Max/Min method eliminates the possibility of multiple freeze-thaw cycles being counted in a single day.

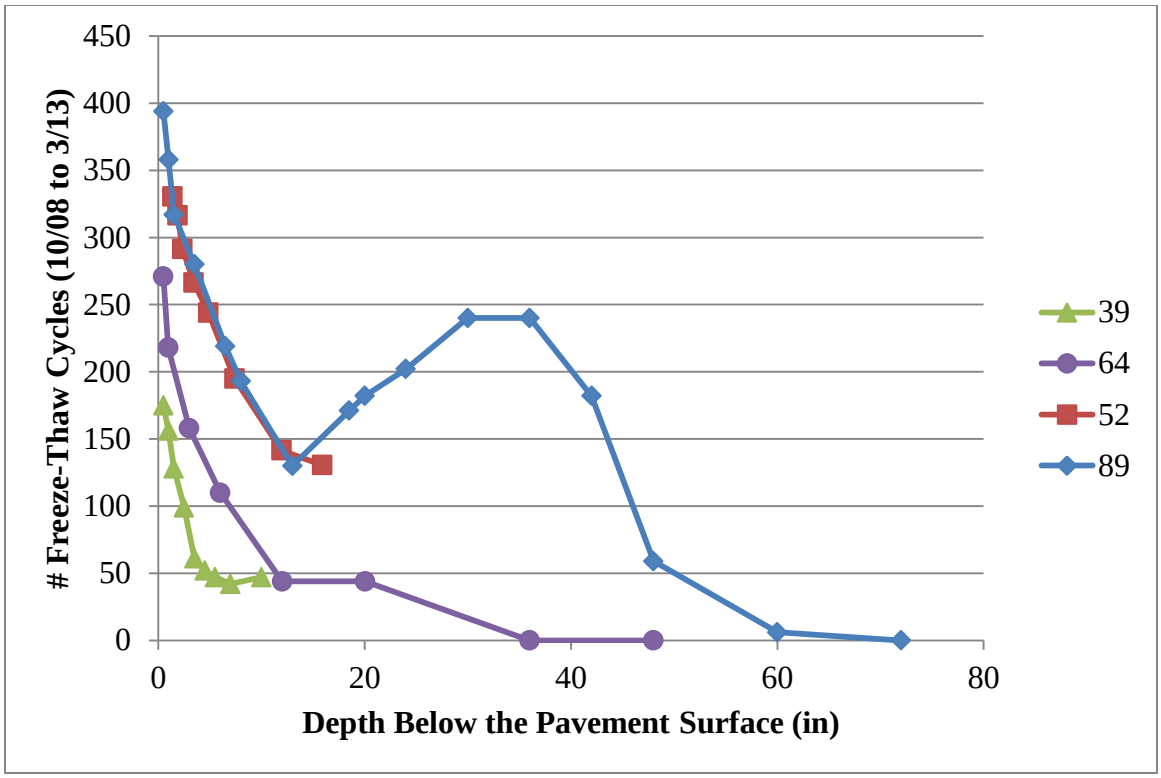

Figure 26: Max/Min Method for Counting Freeze Thaw Cycles

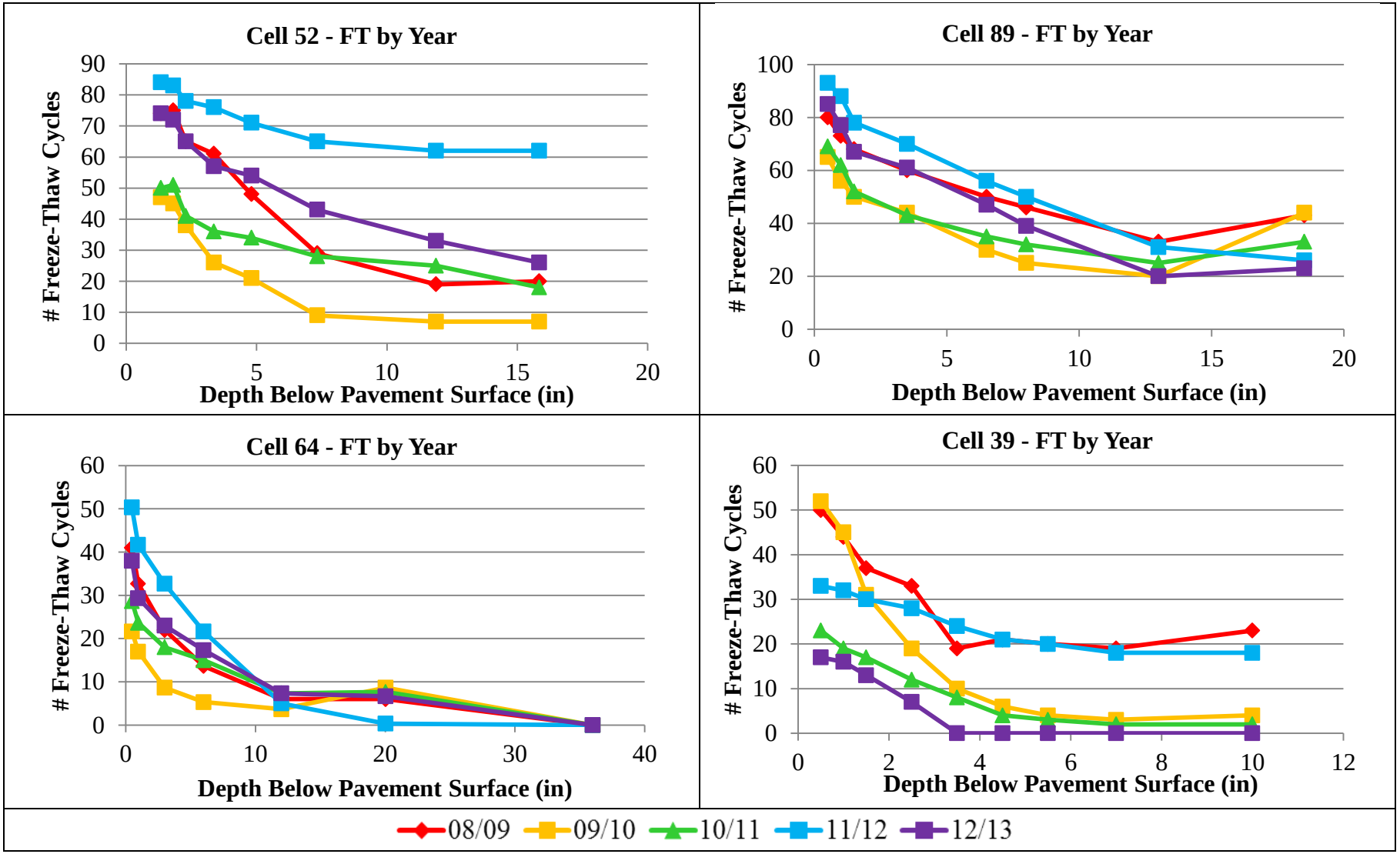

Figure 27: FT By Year – All Cells – Max/Min

Two significant observations are present in the results plotted in Figure 26. First is the nearly equivalent total number of freeze-thaw cycles that were counted in both Cell 52 and Cell 89. As these two cells were similar in thickness and design, this may suggest that pervious concrete does not actually experience fewer freeze-thaw cycles as was originally theorized in the 2009 MnDOT study.

Secondly, there was an interesting increase in total number of freeze-thaw cycles in Cell 89 in the subgrade layer that was not present in the other full-depth pervious test cell (Cell 64). The air voids of the pervious concrete in Cell 64 are likely more clogged than those in Cell 89 due to the earlier (2005), less durable mix designs used in that test cell. Both Cell 89 and Cell 64 have similar base material and clay subgrade.

The increased number of freeze-thaw cycles being detected in the newer, more pervious test cell may suggest the opposite of an insulating effect in the subgrade material. The interconnected air void structure may be allowing more frequent fluctuations in the ambient temperatures to pass through the pervious concrete and be reflected in the temperature swings in the subgrade. Increased moisture levels in the subgrade layer of the pervious concrete may also have an impact on the number of freeze thaw cycles.

Unfortunately, there are no comparable MnROAD impervious concrete test cells that have thermocouple sensors installed at depths past 20 inches and in the subgrade to confirm this theory. However, Cell 54, a 7.5-inch-thick concrete test cell, has a 12-inch aggregate base and clay subgrade, almost identical to the subsurface materials in Cell 89. This test cell was constructed in 2004 using a unique Mesabi-Select coarse aggregate in the concrete (Rhone, 2010). The freeze-thaw cycles were counted in Cell 54 using the Max/Min method to evaluate whether the results would be as similar between cells 54 and 89 as were present between cells 52 and 89. Data was only available for the winter seasons of 08/09, 09/10, and 10/11 for Cell 54. The results are shown in Figure 28 below, where the solid line represents pervious concrete freeze-thaw cycle count, and the dashed lines represent the impervious concrete. Each season is represented by a different color.

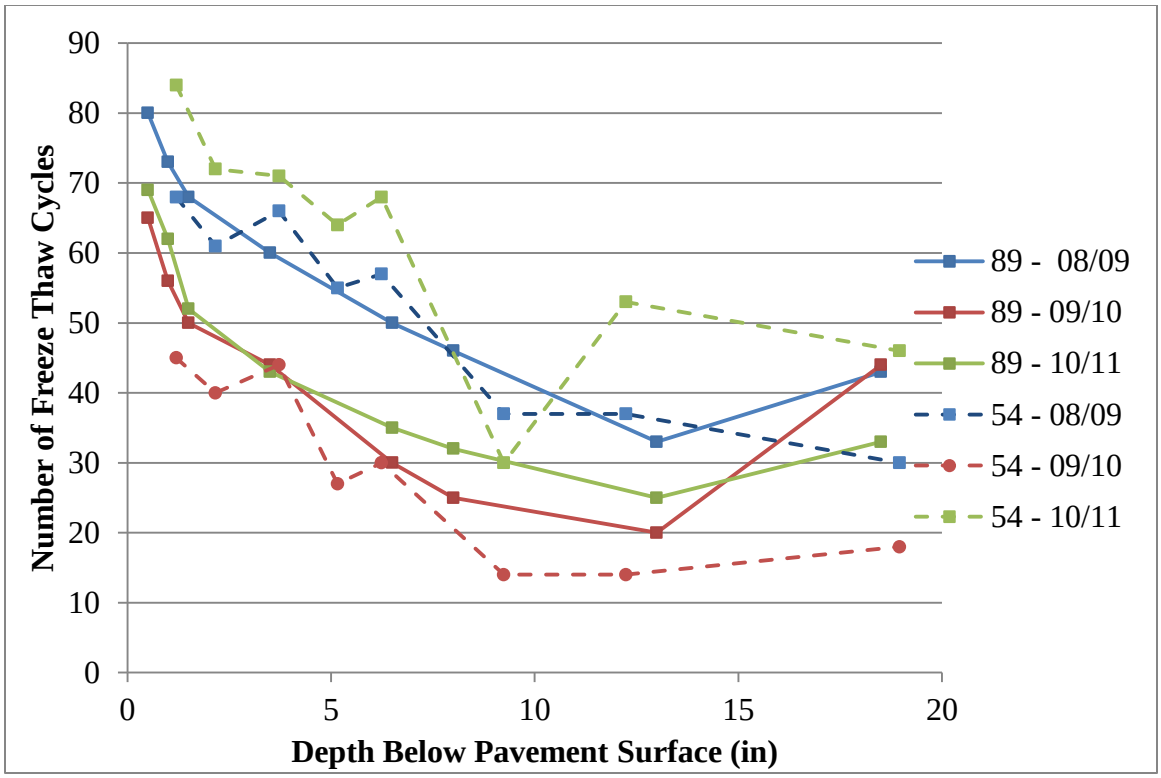

Figure 28: Cell 89 (Pervious) vs. Cell 54 (Impervious) Freeze Thaw – Max/Min

The results show a different pattern for each three seasons. In the first season, the pervious concrete pavement cell has close to the same number of freeze-thaw cycles as the PCC cell. In the second, the pervious concrete pavement has slightly more cycles than the impervious concrete pavement. And finally, in the third winter season, the pervious concrete pavement has significantly fewer freeze-thaw cycles than the impervious concrete pavement. Despite these discrepancies, it may be significant to note that the deepest sensor in the base layer, almost directly above the subgrade, shows a significant increase in the number of freeze-thaw cycles in the pervious concrete cell that is not indicated in the impervious concrete cell.

CHAPTER 8: DISCUSSION AND CONCLUSIONS

This research involved three stages of analysis. The first included analyzing raw temperature data collected from four pervious concrete pavement test cells and one Portland cement concrete pavement test cell to determine in-place thermal diffusivity. This involved developing a MATLAB program that uses the partial differential heat equation to fit a temperature gradient to the data and, in turn, solves for an optimal thermal diffusivity. The second portion of this research involved developing a MATLAB program to perform an uncertainty analysis on the fitted thermal diffusivity results, in addition to validating the optimization program using synthetic data. The final portion of this research involved using the raw thermocouple data to determine the number of freeze-thaw cycles in the five concrete pavement test cells according to two different methods: the 0°C Method and the Max/Min method.

As expected, the pervious concrete pavements analyzed in this research had a significantly lower thermal diffusivity than comparable Portland cement concrete pavement in all cases. The three pervious concrete test cells on the MnROAD Low-Volume Road all had thermal diffusivities around 0.6 ft^2/day, whereas the impervious PCC test cell had an average thermal diffusivity of around 1.7 ft^2/day. Based on the definition of thermal diffusivity as the rate at which temperature changes are made in a material, a lower thermal diffusivity could result in a lower number of freeze-thaw cycles. For example, if the pavement is frozen and ambient temperatures rise above freezing during daylight hours, the pavement temperature at lower depths may not reach above freezing temperatures before ambient temperatures begin to drop again.

All test cells analyzed showed a slight decrease in thermal diffusivity over time. The linear rate of decrease for the impervious concrete test cell is one order of magnitude larger than that of the pervious cells. This decrease could be due to general deterioration or change in the air void structure of the pavements over time.

The pervious concrete test cells were vacuumed and swept twice over the 4.5-year period analyzed in an attempt to remove material from the exposed voids and mitigate clogging of the pavement surface. The thermal diffusivities of the test cells following these

maintenance events did not appear to be affected by any possible changes in the air void structure at the surface of the pavement layer. However, this observation was made after a very limited number of events, and therefore cannot be used to exclude the possibility that maintenance activities such as vacuuming will have an effect on the thermal diffusivity of the pavement.

There were seasonal trends found in the thermal diffusivity values of both the pervious concrete pavement and Portland cement concrete pavement test cells. These seasonal trends may be due to the temperature dependence of thermal properties of concrete. The thermal conductivity of concrete is known to gradually decrease with temperature (Kodur, 2014). One study compiled measured specific heat values of concrete at varying temperatures from multiple different sources and found that the specific heat remains almost constant up to 400 degrees Celsius (Khaliq, 2012). Therefore, based off the relationship $\alpha = k/\rho c_p$ and assuming the density of the concrete remains constant, the thermal diffusivity of concrete would also be inversely related to temperature. The analysis found that diffusivity was lower in the summer months and higher in the winter months, following the inverse relationship to temperature. Another possible explanation for the seasonal trends in thermal diffusivity may be the presence of moisture or stored water within the concrete. The thermal diffusivity of water is much lower than that of concrete (Blumm 2003). Therefore, as there is more water present in the summer months, stored water in the clogged pervious concrete voids may be decreasing the resulting thermal diffusivity value. It is also possible that the large spikes in thermal diffusivity in winter months in some test cells with older thermocouples may also be a result of improperly functioning sensors in the extreme cold temperatures.

A lower thermal diffusivity could theoretically cause atmospheric temperature changes to be reflected more slowly through the depth of the pavement, causing larger temperature gradients. Therefore, the lower thermal diffusivity of the pervious concrete pavements may contribute to an increase in severity of curling of pavement slabs. Curling is caused by a significant temperature difference, or gradient, between the top and bottom of a slab (Abhijeet Gandage et al., 2013). The slab curls upward during the night when the temperatures are cooler towards the surface of the pavement (Nassiri, 2011). Conversely,

the slab curls downward during the day when temperatures are warmer near the surface of the pavement. Since the rigid pavement is not free to curl, this induces tensile stresses in the slab (Nassiri, 2011). These stresses can cause cracking of the slab and, in turn, poor ride quality, especially when combined with additional traffic loads.

The optimization program used to determine the thermal diffusivities was validated using synthetic temperature gradients with a fixed and known diffusivity. The results show that the program was able to identify the diffusivity within a 0.01 percent error. This verifies that the process can successfully determine thermal diffusivity given that the thermal gradient of the material follows the heat equation theory.

As discussed in section 1.3, it has been theorized that pervious concrete pavements may have the ability to reduce the heat island effect. Many common soils have thermal diffusivities around 0.43 ft^2/day (Tuncer, 2000). Based on the results of this study, the pervious concrete test cells had thermal diffusivities only about 41% greater than soil, whereas the impervious concrete test cell had a thermal diffusivity nearly 400% greater than soil. Assuming that surrounding undeveloped areas will heat and cool at a rate relative to the soils' thermal properties, the lower thermal diffusivity of pervious concrete relative to impervious concrete could significantly reduce temperature gradients between developed and undeveloped areas.

An uncertainty analysis was performed to determine how well the heat equation model and resulting thermal diffusivities fit the actual measured temperature gradients. Results for the standard deviation of errors and standard deviation of thermal diffusivity were significantly low, supporting the validity of the model and the fitted thermal diffusivity values. This analysis suggests that the in-place temperature data can be used to accurately determine thermal properties of concrete pavements.

The uncertainty analysis showed a strong seasonal variation in the standard deviation of errors and standard deviation of diffusivity. However, the seasonal trend between the two properties was counterintuitive. Multiple tests were run to verify and explain these surprising results. This could be explained by more drastic temperature swings in the ambient temperatures in the summer months than in the winter. The temperatures

fluctuate more between day and night in the summer, making the boundary conditions highly variable. In turn, a small change in diffusivity will change the solution more drastically in summer than in winter. Therefore, the best fit solution is more dependent on diffusivity in the summer than in the winter.

Preliminary analysis using the 0°C Method for determining freeze-thaw cycles found that all of the pervious concrete pavement test cells had a reduced number of freeze-thaw cycles compared to the typical Portland cement concrete pavement control cell. When using the Max/Min method for determining freeze-thaw cycles, the full-depth pervious concrete pavement cell and the comparable full-depth Portland cement concrete test cell, an almost equal number of cycles were found throughout the pavement and base layers. There was a higher number of freeze-thaw cycles measured in the subgrade layer of the pervious concrete cell than were measured in the base and pavement layer. This suggests that the pervious concrete may not actually be insulating the base and subgrade layers as was theorized in the earlier cited research. Further analysis with new methods for determining frequency of freeze thaw cycles would be beneficial, as the verified diffusivity results suggest that pervious concrete pavement will have significantly different thermal behavior.

One laboratory study conducted at Arizona State University found an approximate range for thermal diffusivity of pervious concrete of between 0.56 and 0.74 (Carlson, 2011). The fitted thermal diffusivity of the in-place pervious concrete in three test cells evaluated in this research consistently fell within this narrow range. This helps to confirm that the thermal behavior of concrete pavements can be accurately described by the heat equation. It also verifies that the MATLAB optimization program developed in this research is a useful and effective tool for determining thermal diffusivity of concrete pavements and can be used in future research to analyze in-place pavement temperature data.

REFERENCES

[1] NRMCA (National Ready Mixed Concrete Association). Freeze Thaw Resistance of Pervious Concrete. Silver Spring, MD. 2004.

[2] Rohne, R., and Izevbekhai, B. MnROAD Cell 64 Pervious Concrete: Third Year Construction Report. Minnesota Department of Transportation. 2009.

[3] Ashley, E. "Using Pervious Concrete to Earn LEED Points." Concrete InFocus. National Ready Mixed Concrete Association. 2008

[4] Towner, J. "Pervious concrete: reducing the heat island effect on parking lot at a time." 2008. <http://azsustainability.com/2008/09/21/pervious-concrete-reducing-the-heat-island-effect-one-parking-lot-at-a-time/> Retrieved November 14 2013.

[5] Wong, E. Reducing Urban Heat Islands: Compendium of Strategies. Climate Protection Partnership Division. U.S. Environmental Protection Agency Office of Atmospheric Programs. 2005.

[6] Nassiri, S. Establishing Permanent Curl/Warp Temperature Gradient in Jointed Plain Concrete Pavements. Doctoral Dissertation, University of Pittsburgh. 2011.

[7] Kaloush, K. Permeable Pavement (Pervious Concrete). 58th Annual Arizona Conference on Roads and Streets. April 10, 2009.

[8] Lamond, J.F. and Pielert, J.H. Significance of Tests and Properties of Concrete and Concrete Making Materials. Issue 169, Part 4. pg. 230. ASTM International. West Conshohocken, PA. 2006.

[9] Rohne, R. Mesabi – Select Concrete Pavement Five Year Performance Report. Minnesota Department of Transportation. 2010.

[10] Carlson, J.D. Pervious Concrete: Questions Answered. Presented to The City of Glendale and the Arizona Cement Association. National Center on SMART Innovations for Urban Climate + Energy, Arizona State University. 2007.

[11] The Michigan Concrete Association. *Pervious Concrete; Porous concrete provides benefits for paving commercial parking lots.* Michigan Contractor and Builder. pp. 12. Print. 2008.

[12] Chen, Y., Wang, K., Wang, X., Zhou, W. Strength, fracture and fatigue of pervious concrete. Construction and Building Materials. Vol.42, pp.97-104. 2013.

[13] Shu, X., Huang, BS., Wu, H., Dong, Q., Burdette, EG. Performance comparison of laboratory and field produced pervious concrete mixtures. Construction And Building Materials, Vol.25 (8), pp.3187-3192. 2011.

[14] Wu, H., Huang, B.S., Shu, X., Dong, Q. Laboratory Evaluation of Abrasion Resistance of Portland Cement Pervious Concrete. Journal of Materials In Civil Engineering. Vol.23. pp.697-702. 2011.

[15] Vancura, M., MacDonald, K., Khazanovich, L. Structural Analysis of Pervious Concrete Pavement. Transportation Research Record. Issue 2226. pp.13-20. 201.1

[16] Henderson, V., Tighe, S. Evaluation of pervious concrete pavement performance in cold weather climates. International Journal Of Pavement Engineering, Vol.13(3), pp.197-208. 2012.

[17] Huang, BS., Wu, H., Shu, X., Burdette, EG. Laboratory evaluation of permeability and strength of polymer-modified pervious concrete. Construction And Building Materials, Vol.24 (5), pp.818-823. 2010.

[18] Henderson, V., Tighe, SL. Evaluation of pervious concrete pavement permeability renewal maintenance methods at field sites in Canada. Canadian Journal Of Civil Engineering, Vol.38(12), pp.1404-1413. 2011.

[19] Claude G. "Air Entrainment versus Air Entrapment." National Precast Concrete Association. December 20, 2012. <http://precast.org/2012/12/air-entrainment-versus-air-entrapment/> Retrieved September 15, 2014.

[20] Environmental Protection Agency. "Pervious Concrete Pavement." Water: Best Management Practices. July 2, 2014. <http://water.epa.gov/polwaste/npdes/swbmp/Pervious-Concrete-Pavement.cfm.> Retrieved September 20, 2014

[21] Sonebi, M., Bassuoni, MT. Investigating the effect of mixture design parameters on pervious concrete by statistical modeling Construction And Building Materials, Vol.38, pp.147-154. 2013.

[22] Kevern, J. T., Wang, K., Schaefer, V. R. Effect of coarse aggregate on the freeze-thaw durability of pervious concrete. Journal of Materials in Civil Engineering. Vol.22 5, p.469. 2010.

[23] Schaefer, V.R., Wang, K., Suleiman, M.T., Kevern, J.T.
Mix Design Development for Pervious Concrete In Cold Weather Climates. Center for Transportation Research and Education. Iowa Department of Transportation. 2006.

[24] Novo, A.V., Bayon, J.R., Castro-Fresno, D., Rodriguez-Hernandez, J. Temperature Performance of Different Pervious Pavements: Rainwater Harvestin g for Energy Recovery Purposes.(Report) Water Resources Management, Vol.27(15), p.5003(14). 2013.

[25] Ferguson, B.K. Porous pavements. CRC Press. Boca Raton, FL. 2005.

[26] Mata, L.A. Sedimentation of pervious concrete pavement systems. North Carolina State University. UMI Dissertations Publishing. 2008.

[27] Suozzo, M.J., Dewoolkar, M.M. Long-Term Field Monitoring and Evaluation of Maintenance Practices for Pervious Concrete Pavement in Vermont. Transportation Research Record: Journal of the Transportation Research Board, Vol.2292(-1), pp.94-103. 2012.

[28] Wanielista, M., Chopra, M. Performance Assessment of Portland Cement Pervious Pavement. Report 2 of 4: Construction and Maintenance Assessment of Pervious Concrete. FDOT Project BD521-02. June 2007. Stormwater Management Academy. University of Central Florida. Orlando, FL 32816.

[29] Radlińska, A., Welker, A., Greising, K., Campbell, B., Littlewood, D. Long-term field performance of pervious concrete pavement. Advances in Civil Engineering, 2012, Vol.2012.

[30] Haselbach, L., Boyer, M., Kevern, JT., Schaefer, VR. Cyclic Heat Island Impacts on Traditional Versus Pervious Concrete Pavement Systems Transportation Research Record, 2011, Issue 2240, pp.107-115.

[31] Increasing exfiltration from pervious concrete and temperature monitoring Tyner, J.S. ; Wright, W.C. ; Dobbs, P.A. Journal of Environmental Management, June 2009, Vol.90(8), pp.2636-2641.

[32] Kevern, J.T., Schaefer, V.R., Wang, K. Temperature behavior of pervious concrete systems. Transportation Research Record, 2009, Issue 2098, pp.94-101. Peer Reviewed Journal.

[33] Bay Area Stormwater Management Agencies Association. “Stormwater control for Small Projects.” City of Los Angeles and Geosyntec Consultants. <http://www.ci.berkeley.ca.us/uploadedFiles/Online_Service_Center/Planning/Stormwater%20Fact%20Sheet_BASMAA_Pervious_Paving.pdf.> Retrieved May 10 2014.

[34] American Concrete Pavement Association. “Stormwater Management with Pervious Concrete Pavement.” <http://www.dep.wv.gov/WWE/Programs/stormwater/MS4/green/Documents/SW%20Mgmt%20with%20pervious%20concrete.pdf.> Retrieved May 10 2014.

[35] Minnesota Pollution Control Agency. “Design Criteria for Permeable Pavement.” <http://stormwater.pca.state.mn.us/index.php/Design_criteria_for_permeable_pavement> Retrieved May 10 2014.

[36] Virginia Department of Environmental Quality. “Permeable Pavement” <http://vwrrc.vt.edu/swc/NonPBMPSpecsMarch11/VASWMBMPSpec7PERMEABLEPAVEMENT.html.> March 2011. Retrieved May 10 2014.

[37] Lemay, L., Lobo, C. “Pervious Concrete: A Solution to Stormwater Runoff.” NMB&CW. September 20, 2011.

[38] Portland Cement Association. “Pervious Concrete and Freeze-Thaw” <http://www.cement.org/for-concrete-books-learning/materials-applications/pervious-concrete/pervious-concrete-and-freeze-thaw.> Retrieved May 15 2014.

[39] Gandage, A.S., Rao, V.R., Vinayaka, Sivakumar, M.V.N., Vasan, A., Venu, M., Yaswanth, A.B. Procedia Effect of Perlite on Thermal Conductivity of Self Compacting Concrete - Social and Behavioral Sciences, 2013, Vol.104, pp.188-197

[40] Washington Aggregates & Concrete Association. “Pervious Concrete.” <http://www.washingtonconcrete.org/pervious-concrete.> Retrieved September 10 2014.

[41] Tang, S., Tang, C. Liang, Z., Zhang, Y., Li, L. Numerical Study of the Influence of Material Structure on Effective Thermal Conductivity of Concrete Heat Transfer Engineering, 2012, Vol.33(8), p.732-747. Peer Reviewed Journal. Taylor & Francis Group.

[42] Shindé, S.L., Goela, J.S. High thermal conductivity materials. New York: Springer. 2006.

[43] Khazanovich, L., Balbo, J.T., Johanneck, L., Lederle, R., Marasteanu, M., Saxena, P., Tompkins, D., Vancura, M., Watson, M., Harvey, J., Santero, N.J., Signore, J. Design and Construction Guidelines for Thermally Insulated Concrete Pavements. January 2013. Department of Civil Engineering, University of Minnesota. Pavement Research, University of California.

[44] Wilde, J. PCC Surface Characteristics – Rehabilitation MnROAD Study. 2013. Center for Transportation Research and Implementation, Minnesota State University Mankato.

[45] Lebens, M.A., Troyer, B. Porous Asphalt Pavement Performance in Cold Regions. Minnesota Department of Transportation. April 2012.

[46] Izevbekhai, B., Akkari, A. Pervious Concrete Cells on MnROAD Low Volume Road. Minnesota Department of Transportation. December 2011.

[47] Morris, A.S., Langari, R. Measurement and instrumentation theory and application.
EngineeringPro. Waltham, MA: Academic Press. 2012.

[48] Van Herwaarden, A.W., Sarro, P.M. Thermal sensors based on the seebeck effect. Sensors and Actuators, Vol.10 (3), pp.321-346. 1986.

[49] Tritt, T. Thermal conductivity theory, properties, and applications. Kluwer Academic/Plenum Publishers, New York. 2004.

[50] Thirumaleshwa, M. Fundamentals of Heat and Mass Transfer. Dorling Kindersley. Patparganj, Delhi. 2006.

[51] Venkanna, B.K. Fundamentals of Heat and Mass Transfer. New Delhi: PHI Learning. p. 38. ISBN 978-81-203-4031-2. 2010.

[52] Kaviany, M. Principles of Heat Transfer. John Wiley & Sons. 2002.

[53] Incropera, F.P., Bergman, T.L., Lavine, A., Dewitt, D.P. Introduction to Heat Transfer, Sixth Edition. John Wiley & Sons, Inc. Hoboken, NJ. 2011.

[54] Fulford, G.R., Broadbridge, P. Industrial Mathematics, Case studies in the diffusion of Heat and Matter. Cambridge University Press. 2002.

[55] Bray, W.A. Journey Into Partial Differential Equations. Jones & Bartlet Learning. Sudbury, MA. 2002.

[56] Banerjee, S. Mathematical Modeling: Models, Analysis and Applications. CRC Press, Taylor & Francis Group. Boca Raton, FL. 2014.

[57] Kodus, V. "Properties of Concrete at Elevated Temperatures," ISRN Civil Engineering, vol. 2014, Article ID 468510, 15 pages. 2014.

[58] Khaliq, W. and Kodur, V. "High temperature mechanical properties of high strength fly ash concrete with and without fibers," ACI Materials Journal, vol. 109, no. 6, pp. 665–674. 2012.

[59] Blumm, J. and Lindemann, A. "Characterization of the thermophysical properties of molten polymers and liquids using the flash technique". High Temperatures-High Pressures. 35/36 (6): 627 - 632. 2007.

[60] Schiesser, W. E. and G. W. Griffiths. A Compendium of Partial Differential Equation Models: Method of Lines Analysis with Matlab, Cambridge University Press. 2009.

[61] Shampine, L.F., Gladwell, I., and Thompson, S. Solving ODEs with MATLAB. Cambridge University Press. New York, NY. 2003.

APPENDIX: SENSOR LOCATION DETAILS

Cell		Sensor ID	Depth (in)	Station	Offset (ft)	Material	Date Installed	Tree #
85	Pervious Concrete Experiment - Low Volume Road - Sand subgrade	1	0.50	16538	-6.6	Pervious Concrete	9/1/08	1
85		2	1.00	16538	-6.6	Pervious Concrete	9/1/08	1
85		3	1.50	16538	-6.6	Pervious Concrete	9/1/08	1
85		4	3.50	16538	-6.6	Pervious Concrete	9/1/08	1
85		5	6.50	16538	-6.6	Pervious Concrete	9/1/08	1
85		6	8.00	16538	-6.6	RR Ballast	9/1/08	1
85		7	13.0	16538	-6.6	CA-15	9/1/08	1
85		8	18.5	16538	-6.6	CA-15	9/1/08	1
85		9	20.0	16538	-6.6	Sand	9/1/08	1
85		10	24.0	16538	-6.6	Sand	9/1/08	1
85		11	30.0	16538	-6.6	Sand	9/1/08	1
85		12	36.0	16538	-6.6	Sand	9/1/08	1
85		13	42.0	16538	-6.6	Sand	9/1/08	1
85		14	48.0	16538	-6.6	Sand	9/1/08	1
85		15	60.0	16538	-6.6	Sand	9/1/08	1
85		16	72.0	16538	-6.6	Sand	9/1/08	1
89	Pervious Concrete Experiment - Low Volume Road - Clay subgrade	17	0.50	17321	-6.5	Pervious Concrete	9/1/08	1
89		18	1.00	17321	-6.5	Pervious Concrete	9/1/08	1
89		19	1.50	17321	-6.5	Pervious Concrete	9/1/08	1
89		20	3.50	17321	-6.5	Pervious Concrete	9/1/08	1
89		21	6.50	17321	-6.5	Pervious Concrete	9/1/08	1
89		22	8.00	17321	-6.5	RR Ballast	9/1/08	1
89		23	13.0	17321	-6.5	CA-15	9/1/08	1
89		24	18.5	17321	-6.5	CA-15	9/1/08	1
89		25	20.0	17321	-6.5	Clay	9/1/08	1
89		26	24.0	17321	-6.5	Clay	9/1/08	1
89		27	30.0	17321	-6.5	Clay	9/1/08	1
89		28	36.0	17321	-6.5	Clay	9/1/08	1
89		29	42.0	17321	-6.5	Clay	9/1/08	1
89		30	48.0	17321	-6.5	Clay	9/1/08	1
89		31	60.0	17321	-6.5	Clay	9/1/08	1
89		32	72.0	17321	-6.5	Clay	9/1/08	1

Cell		Sensor ID	Depth (in)	Station	Offset (ft)	Material	Date Installed	Tree #
39	LVR design PCC - Standard base - longer panel	1	1.20	10056	-0.05	Existing Concrete	7/6/93	1
39		2	3.24	10056	-0.05	Existing Concrete	7/6/93	1
39		3	6.48	10056	-0.05	Existing Concrete	7/6/93	1
39		12	1.08	10054	-9.6	Existing Concrete	7/6/93	2
39		13	3.12	10054	-9.6	Existing Concrete	7/6/93	2
39		14	6.36	10054	-9.6	Existing Concrete	7/6/93	2
39		101	0.50	10039	-6.1	Pervious Concrete	10/17/08	3
39		102	1.00	10039	-6.1	Pervious Concrete	10/17/08	3
39		103	1.50	10039	-6.1	Pervious Concrete	10/17/08	3
39		104	2.50	10039	-6.1	Pervious Concrete	10/17/08	3
39		105	3.50	10039	-6.1	Pervious Concrete	10/17/08	3
39		106	4.50	10039	-6.1	Existing Concrete	10/17/08	3
39		107	5.50	10039	-6.1	Existing Concrete	10/17/08	3
39		108	7.00	10039	-6.1	Existing Concrete	10/17/08	3
39		109	10.0	10039	-6.1	Existing Concrete	10/17/08	3
64	PCC Pervious Concrete Parking Lot- Pole Barn	1	0.48	15	-1	Pervious Concrete	9/22/05	1
64		2	0.96	15	-1	Pervious Concrete	9/22/05	1
64		3	3.00	15	-1	Pervious Concrete	9/22/05	1
64		4	6.00	15	-1	Pervious Concrete	9/22/05	1
64		5	12.0	15	-1	Stone	9/22/05	1
64		6	20.0	15	-1	Clay	9/22/05	1
64		7	36.0	15	-1	Clay	9/22/05	1
64		8	48.0	15	-1	Clay	9/22/05	1
64		9	0.48	30	-1	Pervious Concrete	9/22/05	2
64		10	0.96	30	-1	Pervious Concrete	9/22/05	2
64		11	3.00	30	-1	Pervious Concrete	9/22/05	2
64		12	6.00	30	-1	Pervious Concrete	9/22/05	2
64		13	12.0	30	-1	Stone	9/22/05	2
64		14	20.0	30	-1	Clay	9/22/05	2
64		15	36.0	30	-1	Clay	9/22/05	2
64		16	48.0	30	-1	Clay	9/22/05	2

Cell		Sensor ID	Depth (in)	Station	Offset (ft)	Material	Date Installed	Tree #
52	5 year design PCC - Load testing - FRP dowels	1	1.32	21009	12.48	Concrete	6/17/00	1
52		2	1.80	21009	12.48	Concrete	6/17/00	1
52		3	2.28	21009	12.48	Concrete	6/17/00	1
52		4	3.36	21009	12.48	Concrete	6/17/00	1
52		5	4.80	21009	12.48	Concrete	6/17/00	1
52		6	7.32	21009	12.48	Concrete	6/17/00	1
52		7	11.9	21009	12.48	Gravel	6/17/00	1
52		8	15.8	21009	12.48	Clay	6/17/00	1
52		9	1.44	21016	6.35	Concrete	6/17/00	2
52		10	1.92	21016	6.35	Concrete	6/17/00	2
52		11	2.40	21016	6.35	Concrete	6/17/00	2
52		12	3.48	21016	6.35	Concrete	6/17/00	2
52		13	4.92	21016	6.35	Concrete	6/17/00	2
52		14	7.44	21016	6.35	Concrete	6/17/00	2
52		15	12.0	21016	6.35	Gravel	6/17/00	2
52		16	16.0	21016	6.35	Clay	6/17/00	2